INVARIANTS OF LEGENDRIAN KNOTS AND COHERENT ORIENTATIONS

JOHN B. ETNYRE, LENHARD L. NG, AND JOSHUA M. SABLOFF

Abstract. We provide a translation between Chekanov's combinatorial theory for invariants of Legendrian knots in the standard contact $\mathbb{R}^3$ and a relative version of Eliashberg and Hofer's contact homology. We use this translation to transport the idea of "coherent orientations" from the contact homology world to Chekanov's combinatorial setting. As a result, we obtain a lifting of Chekanov's differential graded algebra invariant to an algebra over $\mathbb{Z}[t, t^{-1}]$ with a full $\mathbb{Z}$ grading.

1. Introduction

Legendrian and transversal knot theory has had an extensive influence on the study of contact 3-manifolds. Early on, Bennequin [3] discovered exotic "overtwisted" contact structures on $\mathbb{R}^3$ using transversal knots. Later authors have used Legendrian and transversal knots to detect overtwisted structures and to construct and distinguish tight ones (see [9, 11, 15, 17], for example). On the topological side, work by Rudolph [20] and others (see [16, 17]) has linked invariants of Legendrian knots of a given knot type with its smooth slicing properties.

In this paper, we will develop tools for distinguishing Legendrian knots in the standard contact $\mathbb{R}^3$. A natural question to ask is whether Legendrian knots in a fixed oriented smooth knot type are classified by their Thurston-Bennequin invariant, tb, and rotation number, r. If so, then we call that smooth knot type **Legendrian simple**. Though it was never widely believed that all knot types were Legendrian simple, early evidence and a lack of suitable invariants suggested that this might be the case. By studying characteristic foliations on spanning disks, Eliashberg and Fraser [7] proved unknots are Legendrian simple in the early 1990s. A few years later, Fuchs and Tabachnikov [13] proved that tb and r are the only finite-type invariants of Legendrian knots. More recently, Etnyre and Honda [10] proved that torus knots and the figure eight knot are also Legendrian simple.

In the mid-1990's, Chekanov [6] developed a method of associating a differential graded algebra (**DGA**) over $\mathbb{Z}/2$ to the xy diagram of a Legendrian knot K. The generators of this DGA correspond to the crossings of the diagram and the differential comes from counting certain immersed polygons whose edges lie in the diagram of the knot and whose vertices lie at the crossings. He proved, combinatorially, that the "stable tame isomorphism class" of the DGA (see Section 3.3 for the precise definition) is invariant under Legendrian isotopy. He then proceeded to find an example of two Legendrian realizations of the 5_2 knot that have the same tb and r, yet are not Legendrian isotopic.

The first goal of this paper is to lift Chekanov's DGA from $\mathbb{Z}/2$ to $\mathbb{Z}[t, t^{-1}]$ coefficients and to provide the DGA with a $\mathbb{Z}$ grading, regardless of the rotation number of the knot.

JBE is partially supported by an NSF Postdoctoral Fellowship (Grant # DMS-0072853).
LLN is partially supported by grants from the NSF and DOE.
JMS is partially supported by an NSF Graduate Student Fellowship and an ARCS Fellowship.

Chekanov's original DGA can be recovered by setting $t = 1$, which will force the grading to be reduced modulo $2r$, and taking the coefficients modulo 2. Part I of the paper is devoted to this goal.

Concurrent with Chekanov's work on his DGA, Eliashberg and Hofer adapted the ideas of Floer homology to the contact setting. Though we will flesh out a relative version of their "contact homology theory" in Section 7, the story goes roughly as follows: let (M, α) be a contact manifold with a Legendrian submanifold K. Let $\mathcal{A}$ be the free associative unital algebra generated by the Reeb chords — i.e. Reeb trajectories that begin and end on K. The generators are graded by something akin to the Maslov index. There is a differential on $\mathcal{A}$ that comes from counting rigid J-holomorphic disks in the **symplectization** $(M \times \mathbb{R}, d(e^\tau \alpha))$ of M. Here, J is a vertically-invariant almost complex structure compatible with $d(e^\tau \alpha)$. Using Floer and Hofer's idea of coherent orientations [8, 12], it is possible to orient all of the moduli spaces of rigid J-holomorphic disks used in the definition of the differential. As a result, we may use $\mathbb{Z}$ coefficients in the definition of the algebra $\mathcal{A}$.

The second goal of this paper, carried out in Part II, is to prove that Chekanov's DGA, and our generalization of it, is a combinatorial translation of relative contact homology. Knowing the relation between the combinatorial and geometric versions of contact homology is quite useful. In particular, the lifting of Chekanov's DGA from $\mathbb{Z}/2$ to $\mathbb{Z}[t, t^{-1}]$ was accomplished by studying this relationship. Moreover, explicit computations in the framework of Eliashberg and Hofer's contact homology theory can be difficult, while computations in the combinatorial theory are more straightforward. Thus, our translation between the two theories yields many explicit computations in contact homology.

The paper consists of essentially two parts. After recalling several basic ideas from contact geometry in Section 2, we proceed, in Part I, to describe the combinatorial theory. This part is self-contained apart from a few technical proofs that are relegated to an appendix of Part I. In Part II of the paper we discuss Eliashberg and Hofer's contact homology and coherent orientations. We then prove the combinatorial theory developed in Part I is a faithful translation of this more geometric theory.

2. Basic Notions

We begin by describing some basic notions in three-dimensional contact geometry. A **contact structure** on a 3-manifold M is a completely non-integrable 2-plane field ξ. Locally, a contact structure is the kernel of a 1-form α that satisfies the following non-degeneracy condition at every point in M:

$$\alpha \wedge d\alpha \neq 0.$$

In this paper, we will be interested in the standard contact structure ξ_0 on $\mathbb{R}^3$, which is defined to be the kernel of the 1-form

$$\alpha_0 = dz + x\, dy.$$

To each contact form α, we may associate a **Reeb field** X_α that satisfies $d\alpha(X_\alpha, \cdot) = 0$ and $\alpha(X_\alpha) = 1$. By Darboux's theorem, every contact manifold is locally contactomorphic to $(\mathbb{R}^3, \xi_0)$. See [2, chapter 8] for an introduction to the fundamentals of contact geometry.

Our primary objects of study are **Legendrian knots** in $\mathbb{R}^3$, i.e. knots that are everywhere tangent to the standard contact structure ξ_0. In particular, we examine Legendrian isotopy classes of Legendrian knots, in which two knots are deemed equivalent if they are related by an isotopy through Legendrian knots.

Legendrian knots are plentiful: it is not hard to prove that any smooth knot can be continuously approximated by a Legendrian knot. Put another way, every smooth knot type has a Legendrian representative. The interactions between Legendrian and smooth knot types constitute a rich and subtle subject. The first step in analyzing this interaction is to introduce the "classical" invariants tb and r for Legendrian knots in $(\mathbb{R}^3, \xi_0)$. (See [2, chapter 8] for more general definitions than we give here.) The **Thurston-Bennequin** invariant measures the self-linking of a Legendrian knot K. More precisely, let K' be a knot that has been pushed off of K in a direction tangent to the contact structure. Define $tb(K)$ to be the linking number of K and K'. The **rotation number** r of an oriented Legendrian knot K is the rotation of its tangent vector field with respect to any global trivialization of ξ_0 (e.g. $\{\partial_x, \partial_y - x\,\partial_z\}$).

In this paper, we use the combinatorics of generic projections of Legendrian knots into the xy plane extensively. Not all knot diagrams in the xy plane can be lifted to Legendrian knots: Stokes' Theorem implies that the diagram must bound zero (signed) area. Chekanov describes the combinatorial restrictions on the form of the xy projection of a Legendrian knot in [6]. Note that the Thurston-Bennequin number of K may be computed from the writhe of the xy projection of K while the rotation number of K is just the (counterclockwise) rotation number of the diagram. For example, the Legendrian unknot in Figure 4 has $tb = -2$ and $r = 1$.

Part I
The Combinatorial Theory

In Section 3 of the paper we describe the contact homology of a knot in $\mathbb{R}^3$ in purely combinatorial terms. We do this by giving a self-contained generalization of Chekanov's differential graded algebra. In broad outline we follow [6], making the necessary changes to extend the DGA defined there over $\mathbb{Z}/2$ to a DGA over $\mathbb{Z}[t, t^{-1}]$. We provide several illustrative computations in Section 4.

3. A Combinatorial Definition of the Algebra

Given an oriented Legendrian knot K in standard contact structure on $\mathbb{R}^3$ we show how to associate a differential graded algebra over $\mathbb{Z}[t, t^{-1}]$ to it in Sections 3.1 and 3.2. Then, in Section 3.3, we describe an equivalence relation, stable tame isomorphism, on DGA's and show that the equivalence class of the DGA associated to a Legendrian knot is invariant under Legendrian isotopy. This in turn implies that the homology of the DGA is invariant under Legendrian isotopy. The algebras and homology that we work with are non-abelian and hence somewhat hard to use. In Section 3.4 we prove that when the DGA of a Legendrian knot is abelianized (over $\mathbb{Q}$), its homology is still invariant under Legendrian isotopy.

3.1. From the Knot K to the Algebra $\mathcal{A}$.

We begin by decorating a generic xy diagram of a given Legendrian knot K. First, label the crossings of K by $\{a_1, \ldots, a_n\}$. Next, label each quadrant around a crossing as shown in Figure 1. We will refer to these labels as the **Reeb signs**. Call a quadrant at a crossing **positive** or **negative** depending on its Reeb sign.

Definition 3.1. The algebra $\mathcal{A}(a_1, \ldots, a_n)$ is the graded free associative unital algebra over $\mathbb{Z}[t, t^{-1}]$ generated (as an algebra) by $\{a_1, \ldots, a_n\}$.

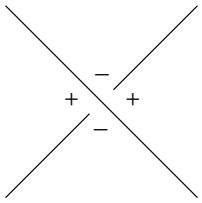

FIGURE 1. The Reeb signs around a crossing.

FIGURE 2. The choice of capping path γ for a crossing. The path γ is denoted by a heavy line; the arrows indicate the orientation of the knot and of γ; and the signs are Reeb signs. The diagrams show a crossing coherent about a + and about a −, respectively.

The grading for t is defined to be $2r(K)$. To grade a generator a_i, we first need to specify a capping path γ_{a_i}. By this we mean the unique path γ_{a_i} in K which begins at the undercrossing of a_i, follows in the direction of the orientation of K, and ends when it reaches the overcrossing of a_i; see Figure 2. Let the rotation number $r(\gamma_{a_i})$ be the fractional number of counterclockwise revolutions made by a tangent vector to γ_{a_i} as we traverse the path. (Thus the rotation number of the entire oriented knot K is the usual rotation number.) We may perturb the diagram of K so that all crossings are orthogonal; then $r(\gamma_{a_i})$ is an odd multiple of $1/4$. Define

$$|a_i| = -2r(\gamma_{a_i}) - \frac{1}{2}. \tag{3.1}$$

In addition, define the **sign of a crossing** a_i to be $\operatorname{sgn} a_i = (-1)^{|a_i|}$. (Note that we may recover Chekanov's original grading by setting $t = 1$, but this forces us to consider the grading modulo $2r(K)$.)

We need one more piece of notation. Define a_i to be **coherent about a** + (respectively **coherent about a** −) if, in a neighborhood of a_i, the quadrant enclosed by the path γ_{a_i} is labeled by a + (resp. −). We also say that the quadrants that are enclosed by γ_{a_i} or its complement are **coherent**; the remaining two quadrants are **incoherent**. The following lemma will be useful in the future.

Lemma 3.2. *If a crossing is coherent about a + (resp. −), then the grading of the associated variable a_i is odd (resp. even).*

Proof. For a crossing coherent about a +, the rotation number of γ is $k - \frac{3}{4}$ for some integer k (see Figure 2); then by definition,

$$|a_i| = -2(k - \frac{3}{4}) - \frac{1}{2} = -2k + 1. \tag{3.2}$$

The proof for the other case is identical. □

3.2. **The Differential ∂.** We describe the differential ∂ by appropriately counting immersed disks in the xy-projection of K. For this, we need some notation. Let $D^2_* = D^2 \setminus \{x, y_1, \dots, y_n\}$, where $\{x, y_1, \dots, y_n\} \subset \partial D^2$ are called boundary punctures. Throughout this section, $\mathbb{R}^2$ refers to the xy-plane.

Definition 3.3. Fix a homology class $A \in H_1(K) = \mathbb{Z}$ and define $\Delta^A(a; b_1, \dots, b_n)$ to be the space of all orientation-preserving immersions $f : (D^2_*, \partial D^2_*) \to (\mathbb{R}^2, K)$ (up to reparametrization) that satisfy:

(1) The homology class $\left[(\pi_{xy}|_K)^{-1}\left(\mathrm{Im}(f|_{\partial D^2}) \cup \gamma_a \cup -\gamma_{b_1} \cup \cdots \cup -\gamma_{b_n}\right)\right]$ coincides with A.
(2) The map f sends the boundary punctures to the crossings of the diagram of K, and at a boundary puncture, the map f covers either one or three quadrants, with the majority of the quadrants positive at the crossing a and negative at the crossings b_i.

Formally, we define the dimension of $\Delta^A(a; b_1, \dots, b_n)$ to be

$$\dim(\Delta^A(a; b_1, \dots, b_n)) = |a| - \sum |b_i| + 2n(A)r(K) - 1, \tag{3.3}$$

where $n(A) \in \mathbb{Z}$ is the image of A under the isomorphism $H_1(K) \cong \mathbb{Z}$ given by the choice of orientation for K.

We call a boundary puncture of f a **convex** or **non-convex corner**, depending on whether f covers one or three quadrants, respectively, at the puncture. The formal dimension of $\Delta^A(a; b_1, \dots, b_n)$ dictates the number of non-convex corners of elements of $\Delta^A(a; b_1, \dots, b_n)$.

Lemma 3.4. *Any $f \in \Delta^A(a; b_1, \dots, b_n)$ has precisely $\dim(\Delta^A(a; b_1, \dots, b_n))$ non-convex corners.*

Proof. Suppose that f has k non-convex corners. Let γ be the closed curve in the diagram of K which is the union of the oriented boundary $f(\partial D^2)$ and the paths $\gamma_a, -\gamma_{b_1}, \dots, -\gamma_{b_n}$. Then the rotation number of γ is, by definition, $n(A)r(K)$.

On the other hand, the rotation number of γ is also the sum of the rotation numbers of its pieces. We may assume that the crossings of the diagram of K are orthogonal. The sum of the rotation numbers of the smooth pieces of γ is simply $1 - (n + 1 - 2k)/4$, because γ is traversed counterclockwise, and each corner contributes a rotation of $1/4$ if convex, and $-1/4$ if non-convex. Also, the rotation number of γ_a is $-(2|a| + 1)/4$, and similarly for γ_{b_i}. Thus the rotation number of γ is

$$n(A)r(K) = 1 - \frac{n + 1 - 2k}{4} - \frac{2|a| + 1}{4} + \sum_{i=1}^{n} \frac{2|b_i| + 1}{4} = \frac{-|a| + \sum |b_i| + k + 1}{2}. \tag{3.4}$$

This implies that $k = \dim(\Delta^A(a; b_1, \dots, b_n))$, as desired. □

We can assign a word in $\mathcal{A}$ to each immersed disk as follows: starting with the first corner after the one covering the + quadrant, the word is a list of the crossing labels of all subsequent negative corners encountered while traversing the boundary of the immersed polygon counter-clockwise. We also associate a sign to each immersed disk as follows:

Definition 3.5. To each quadrant Q in the neighborhood of a crossing a, we associate a sign $\varepsilon_{Q,a}$, called the **orientation sign**, determined from Figure 3. For an immersed disk with one positive corner a (with respect to the Reeb signs) and negative corners $b_1, \dots, b_n$,

FIGURE 3. The signs in the figures are Reeb signs. The orientation signs are -1 for the two shaded quadrants and $+1$ elsewhere.

define the orientation sign $\varepsilon(a; b_1, \ldots, b_n)$ to be the product of the orientation signs over all corners of the disk.

Inspection of Figure 3 yields the following lemma, which will be useful in Sections 5 and 6 when we prove that ∂ is a differential and $\mathcal{A}$ is invariant under Legendrian isotopy.

Lemma 3.6. *Around a crossing a, the product of the orientation signs of two opposite quadrants is $-\operatorname{sgn} a$. The product of the orientation signs of two adjacent quadrants is 1 or $-\operatorname{sgn} a$, depending on whether the Reeb signs of the two quadrants are, in counterclockwise order around the crossing, $-$ and $+$ or $+$ and $-$, respectively. (These cases correspond to the quadrants being on the same side of the undercrossing or overcrossing line, respectively.)*

We are ready to define a differential on $\mathcal{A}$.

Theorem 3.7. *The algebra $\mathcal{A}$ is a differential graded algebra (DGA) whose differential ∂ is defined as follows:*

$$\partial a = \sum_{\dim(\Delta^A(a;b_1,\ldots,b_n))=0} \varepsilon(a; b_1, \ldots, b_n) t^{-n(A)} b_1 \cdots b_n. \tag{3.5}$$

Extend ∂ to $\mathcal{A}$ via $\partial(\mathbb{Z}[t, t^{-1}]) = 0$ and the signed Leibniz rule:

$$\partial(vw) = (\partial v)w + (-1)^{|v|} v(\partial w). \tag{3.6}$$

The differential ∂ has degree -1 and satisfies $\partial^2 = 0$.

We remark that Lemma 3.4 implies that the sum in equation (3.5) is over immersions with no non-convex corners. Note that we use $t^{-n(A)}$ rather than $t^{n(A)}$ in equation (3.5); this convention simplifies notation slightly in examples.

The fact that ∂ has degree -1 follows directly from the dimension formula, equation (3.3). To prove Theorem 3.7, it suffices to check that $\partial^2 = 0$; this is done in Section 5.

3.3. **Algebraic Definitions.** The definition of $\mathcal{A}$ depends heavily on the choice of the projection of K. The following definitions, due essentially to Chekanov [6], give a notion of equivalence which reflects the possible changes in $\mathcal{A}$ due to changes in the knot projection under Legendrian isotopy.

The first definition picks out a particularly simple set of isomorphisms of $\mathcal{A}$.

Definition 3.8. A graded chain isomorphism

$$\phi : \mathcal{A}(a_1, ..., a_n) \longrightarrow \mathcal{A}(b_1, \dots, b_n)$$

is **elementary** if there is some $j \in \{1, \dots, n\}$ such that

$$\phi(a_i) = \begin{cases} b_i, & i \neq j \\ \pm b_j + u, & u \in \mathcal{A}(b_1, \dots, b_{j-1}, b_{j+1}, \dots, b_n),\ i = j. \end{cases} \tag{3.7}$$

A composition of elementary isomorphisms is called **tame**.

We note that since it is not known whether or not all isomorphisms are tame we should technically be working with "semi-free" algebras (free algebras with specified generators). This technical point will not cause any problems so we ignore it. In [6], this point is carefully discussed and the interested reader is referred there.

We also need an algebraic operation that reflects the second Reidemeister move (see move III in Figure 7). Define a special algebra $\mathcal{E}_i = \mathcal{A}(e_1, e_2)$ by setting $|e_1| = i$, $|e_2| = i - 1$, $\partial e_1 = e_2$, $\partial e_2 = 0$.

Definition 3.9. The degree i **stabilization** $S_i(\mathcal{A}(a_1, \dots, a_n))$ of $\mathcal{A}(a_1, \dots, a_n)$ is defined to be $\mathcal{A}(a_1, \dots, a_n, e_1^i, e_2^i)$. The grading and the differential are inherited from both $\mathcal{A}$ and $\mathcal{E}_i$. Two algebras $\mathcal{A}$ and $\mathcal{A}'$ are **stable tame isomorphic** if there exist two sequences of stabilizations $S_{i_1}, \dots, S_{i_n}$ and $S_{j_1}, \dots, S_{j_m}$ and a tame isomorphism

$$\phi : S_{i_n}(\cdots S_{i_1}(\mathcal{A}) \cdots) \longrightarrow S_{j_m}(\cdots S_{j_1}(\mathcal{A}') \cdots).$$

Two differential algebras $(\mathcal{A}; \partial)$ and $(\mathcal{A}'; \partial')$ are **stable tame isomorphic** if there is a stable tame isomorphism from $\mathcal{A}$ to $\mathcal{A}'$ that is also a chain map.

This equivalence relation is designed for the following important theorem.

Theorem 3.10. *The stable tame isomorphism class of $\mathcal{A}(a_1, \dots, a_n; \partial)$ is invariant under Legendrian isotopy of K.*

Chekanov proved this theorem over $\mathbb{Z}/2$; we will prove the $\mathbb{Z}[t, t^{-1}]$ version of this theorem in Section 6. As a corollary, we obtain a proof that the homology of $\mathcal{A}(a_1, \dots, a_n; \partial)$ is an invariant:

Corollary 3.11. *The homology $H(\mathcal{A}(a_1, \dots, a_n; \partial))$ is invariant under Legendrian isotopy of K.*

Proof. It suffices to prove that homology does not change under stabilizations. Consider the natural inclusion and projection

$$\mathcal{A} \xrightarrow{i} S(\mathcal{A}) \xrightarrow{\tau} \mathcal{A}.$$

On one hand, $\tau \circ i = Id_{\mathcal{A}}$. We need to prove that $i \circ \tau$ is chain homotopic to $Id_{S(\mathcal{A})}$, i.e. that there exists some linear map $H : S(\mathcal{A}) \to S(\mathcal{A})$ that satisfies

$$i \circ \tau - Id_{S(\mathcal{A})} = H \circ \partial + \partial \circ H. \tag{3.8}$$

It is not hard to check that the following H satisfies these requirements:

$$H(w) = \begin{cases} 0 & w \in \mathcal{A} \\ 0 & w = ae_1b \quad \text{with } a \in \mathcal{A} \\ (-1)^{|a|+1} ae_1 b & w = ae_2b \quad \text{with } a \in \mathcal{A}. \end{cases} \tag{3.9}$$

□

3.4. **Abelianization of $\mathcal{A}$.** One possible way to simplify calculations with $\mathcal{A}$ is to change the base ring and abelianize.

Definition 3.12. Given a Legendrian knot K with crossings labeled $\{a_1, \dots, a_n\}$, let $\tilde{\mathcal{A}}_{\mathbb{Q}}(a_1, \dots, a_n; \partial)$ be the free graded supercommutative associative unital differential algebra over $\mathbb{Q}[t, t^{-1}]$ generated as an algebra by $\{a_1, \dots, a_n\}$. The gradings and the differential ∂ are the same as those defined in Section 3.2.

By supercommutative we mean that $wv = (-1)^{|v||w|}vw$. A key feature of the abelianized algebra over a field not of characteristic 2 is that for any generator a of odd degree, $a^2 = 0$. Note that this is not the case if we abelianize over $\mathbb{Z}/2$.

Just as in the non-abelian case, we have the following results (cf. Theorem 3.10 and Corollary 3.11).

Proposition 3.13. *The stable tame isomorphism class of $\tilde{\mathcal{A}}_{\mathbb{Q}}$ is an invariant of the Legendrian isotopy class of the Legendrian knot K.*

The proof of 3.13 is a simple diagram chase.

Theorem 3.14. *The homology of $\tilde{\mathcal{A}}_{\mathbb{Q}}$ is an invariant of the Legendrian isotopy class of the Legendrian knot K.*

Proof. The only place where we use the non-commutativity of $\mathcal{A}$ in proving invariance is in the definition of the map H in Corollary 3.11. In the abelianized case over $\mathbb{Q}$, we can redefine H so that it is still a chain homotopy.

If i is even, then we define $H : S_i(\tilde{\mathcal{A}}) \to S_i(\tilde{\mathcal{A}})$ as follows:

$$H(w) = \begin{cases} -\frac{1}{k+1}e_1^{k+1}a & w \in e_2e_1^k\tilde{\mathcal{A}}(a_1, \dots, a_n) \\ 0 & \text{otherwise;} \end{cases} \tag{3.10}$$

if i is odd,

$$H(w) = \begin{cases} -e_2^{k-1}e_1\tilde{a} & w \in e_2^k\tilde{\mathcal{A}}(a_1, \dots, a_n, e_1) \\ 0 & \text{otherwise.} \end{cases} \tag{3.11}$$

It is easy to check that this H works in the abelianized version of the proof of Corollary 3.11. □

4. Examples

In this section, we compute the DGA for three sample knots with both orientations.

4.1. **Unknot.** Consider the oriented unknot in Figure 4 which has $tb = -2$ and $r = 1$. The capping paths are given by $\gamma_a = \gamma_1$ and $\gamma_b = \gamma_4 + \gamma_1 + \gamma_2$. Assuming orthogonal crossings gives $r(\gamma_a) = -3/4$ and $r(\gamma_b) = 1/4$; hence $|a| = 1$, $|b| = -1$, and $|t| = 2$.

The word in ∂a represented by the immersed disk shown in Figure 4 is is tb^2, where the power of t follows from the fact that the boundary of the disk is $\gamma = \gamma_2 - \gamma_3 + \gamma_4$, and $\gamma + \gamma_a - 2\gamma_b$ winds -1 times around the knot.

Continuing in this way, we find that $\partial a = 1 + tb^2$, $\partial b = t^{-1}$. Note that all orientation signs are positive, because both crossings are odd degree and hence coherent about a $+$. Since t has degree 2, we see that ∂ does indeed lower degree by 1.

If we reverse the orientation of the knot, we may similarly compute that $r = -1$, $|a| = 3$, $|b| = 1$, $\partial a = t^{-1} + b^2$, $\partial b = 1$.

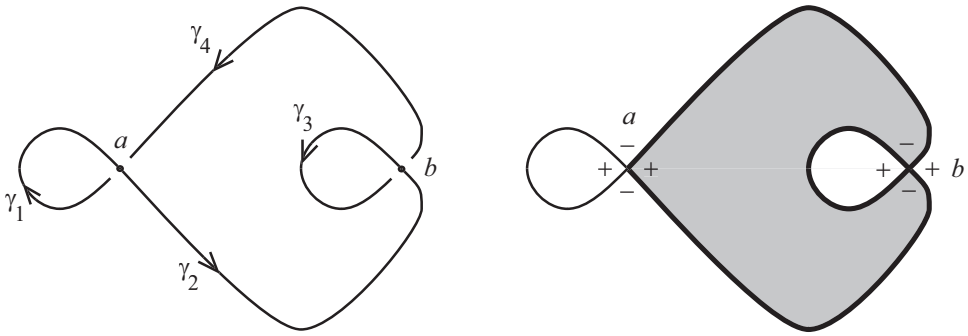

FIGURE 4. The unknot with $tb = -2$ and $r = 1$. On the left, the knot has been divided by crossings a and b into four oriented curves. On the right, Reeb signs and an embedded disk are shown.

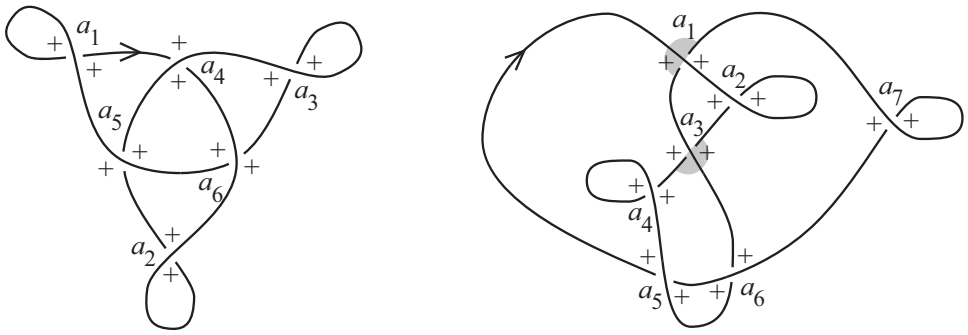

FIGURE 5. Examples of Legendrian trefoil and figure eight knots. Crossings are labeled, and the + signs represent Reeb signs; to reduce clutter, the − Reeb signs have been omitted. The four shaded quadrants are the only quadrants with negative orientation sign.

This knot is reducible, in the terminology of [6]; that is, we can view it as a Legendrian knot with an added loop (the loop around b). As in [6], any reducible knot has a DGA with trivial homology, and which indeed contains no information besides the classical invariants. In our case, for the original orientation, $\partial(tb) = 1$, and so the homology vanishes.

4.2. **Trefoil.** Consider the right-handed trefoil knot depicted in Figure 5. (This is example 4.3 in [6].) This satisfies $r = 1$, $tb = -6$, and $|a_i| = -1$ for all i. As in the previous example, all orientation signs are positive.

We can then compute the differential:

$$\begin{aligned} \partial a_1 &= t^{-1} + a_5 a_4 \\ \partial a_2 &= t^{-1} + a_6 a_5 \\ \partial a_3 &= t^{-1} + a_4 a_6 \\ \partial a_4 &= \partial a_5 = \partial a_6 = 0. \end{aligned}$$

Note that, for this knot or any knot with $r \neq 0$, it is easiest to deduce powers of t from the facts that t has degree $2r$ and ∂ lowers degree by 1.

For the same knot with the opposite orientation, we have $r = -1$, $|a_i| = 1$ for all i, and

$$\begin{aligned} \partial a_1 &= 1 + ta_5a_4 \\ \partial a_2 &= 1 + ta_6a_5 \\ \partial a_3 &= 1 + ta_4a_6 \\ \partial a_4 &= \partial a_5 = \partial a_6 = 0. \end{aligned}$$

4.3. **Figure eight.** Consider the figure eight knot depicted in Figure 5. We have $r = 0$ and $tb = -3$, and the degrees of the crossings are given by $|a_2| = |a_4| = |a_5| = |a_7| = 1$, $|a_1| = |a_3| = 0$, $|a_6| = -1$.

A tip for calculating powers of t, especially for knots with $r = 0$: it is useful to choose a small section of the knot and count how many times it is traversed by the boundary of the immersed disk and the capping paths. For instance, for the figure eight knot, the loop next to a_7 is traversed (positively) by the capping paths for a_1, a_2, and a_6. Thus the exponent of t for a monomial in ∂a_i is the number of times a_1, a_2, a_6 appears in the monomial, minus one if $i = 1, 2, 6$; for the term 1 in ∂a_7 only, we must then subtract one, since this is the only disk whose boundary traverses (positively) the loop next to a_7.

We thus find that

$$\begin{aligned} \partial a_1 &= -a_6 + a_6a_3 + ta_6a_3a_5a_6 & \qquad \partial a_4 &= 1 - a_3 - ta_5a_6a_3 \\ \partial a_2 &= t^{-1} + a_1a_3 - a_6a_3a_4 & \qquad \partial a_7 &= t^{-1} + a_3 - ta_3a_6a_3a_5 \\ & \partial a_3 = \partial a_5 = \partial a_6 = 0. \end{aligned}$$

For the knot with the opposite orientation, the degrees of the crossings remain the same since $r = 0$, but the signs and powers of t in the differential change:

$$\begin{aligned} \partial a_1 &= a_6 + ta_6a_3 + ta_6a_3a_5a_6 & \qquad \partial a_4 &= t^{-1} + a_3 + ta_5a_6a_3 \\ \partial a_2 &= 1 + ta_1a_3 + t^2a_6a_3a_4 & \qquad \partial a_7 &= 1 - a_3 - t^2a_3a_6a_3a_5 \\ & \partial a_3 = \partial a_5 = \partial a_6 = 0. \end{aligned}$$

Appendix to Part I
Proofs of $\partial^2 = 0$ and Invariance

Here we show that the arguments in [6] can be strengthened to prove Theorems 3.7 and 3.10.

5. Proof that $\partial^2 = 0$

The geometric motivation behind the following proof will become clear in Section 7. For now, we give a purely combinatorial proof that $\partial^2 = 0$. Our proof mimics the corresponding proof in [6], so we omit some details and cases but clearly indicate the complications added by our signs and powers of t.

Since ∂ obeys the signed Leibniz rule, it suffices to prove that $\partial^2 = 0$ on the generators of $\mathcal{A}$. Let a be such a generator. If we disregard signs and powers of t for now, a term in $\partial^2 a$ is of the form

$$a_1 \cdots a_k b_2 \cdots b_l c_1 \cdots c_m, \tag{5.1}$$

where $a_1 \cdots a_k b_1 c_1 \cdots c_m$ and $b_2 \cdots b_l$ are terms in ∂a and ∂b_1, respectively. We may think of this term in $\partial^2 a$ as the two relevant disks glued together at the crossing b_1; see Figure 6. Gluing yields a loop that has a branch point just after the corner at b_l.

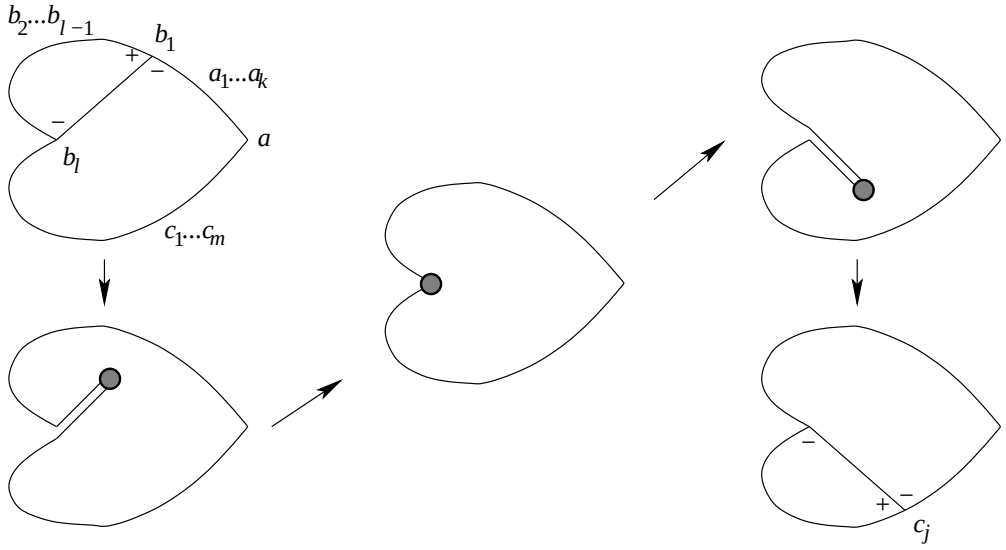

FIGURE 6. One possible configuration for disks involved in $\partial^2 a$. The signs are Reeb signs.

After retracting the branch point to the boundary of the obtuse disk (in Figure 6, we retract to b_l), we may think of this loop as the boundary of an "obtuse disk," i.e., a disk with exactly one non-convex corner. Near the non-convex corner, there are two segments of K pointing into the obtuse disk; we have just pushed the branch point along one of these segments. Now push it along the other segment, and continue until the loop breaks into the boundary of two immersed disks; see Figure 6. These two immersed disks represent another term contributing to $\partial^2 a$ which cancels our original term, up to signs and powers of t. To complete the proof that $\partial^2 = 0$, we need to check that our two terms share the same power of t and have opposite signs.

We first address the powers of t. As described in Section 3.2, the (counterclockwise oriented) boundary of each disk, along with the appropriately oriented capping paths of the corners of the disk, forms a closed curve in K; the negation of the winding number of this curve around K is the power of t associated to the disk. For two disks which glue together to form an obtuse disk, a quick consideration of the capping paths shows that the powers of t associated to the two disks multiply to give the power of t associated to the obtuse disk. Hence the two terms of $\partial^2 a$ corresponding to a given obtuse disk have the same power of t.

It remains to check that the two terms in $\partial^2 a$ corresponding to a fixed obtuse disk have opposite signs. Consider the obtuse disk D in Figure 6, with positive corner at a and non-convex corner at b_l. For two points v_1, v_2 along the boundary of this disk, let sgn $\overline{v_1 v_2}$ denote the product of sgn w over all corners w on the portion of the boundary from v_1 to v_2, not including the endpoints; here the boundary is oriented counterclockwise.

There are several possible configurations, depending on how the paths from b_l divide D. We will consider one such configuration, shown in Figure 6; the arguments for the other configurations are similar.

The two terms in $\partial^2 a$ arising from D have two sets of signs: one from the disks themselves through Definition 3.5, and one from the signed Leibniz rule. The signs arising from the signed Leibniz rule are sgn $\overline{ab_1}$ for the figure at the top left and sgn $\overline{ab_l}$ for the figure on the bottom right. The signs arising from the disks themselves are the same for both

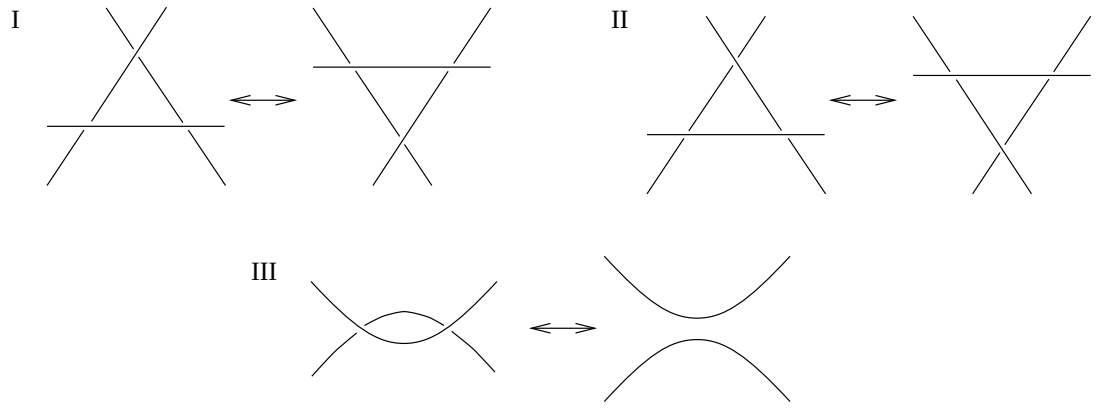

FIGURE 7. The three Legendrian Reidemeister moves.

figures, with the exception of the contribution of the corners marked with their Reeb signs in Figure 6.

Lemma 3.6 applied to Figure 6 shows that the total contribution of the marked corners at b_1, b_l, and c_j is $-\text{sgn } b_1$, $-\text{sgn } b_l$, and 1, respectively. Hence the total sign difference between the two terms in $\partial^2 a$ is

$$(\text{sgn } \overline{ab_1})(\text{sgn } \overline{ab_l})(-\text{sgn } b_1)(-\text{sgn } b_l) = (\text{sgn } b_1)(\text{sgn } \overline{b_1 b_l})(\text{sgn } b_l) = -1, \tag{5.2}$$

where the last equality follows from the fact that ∂ lowers degree by 1.

This concludes the checking of signs, and the proof that $\partial^2 = 0$. Theorem 3.7 follows. □

6. Invariance of $\mathcal{A}$

The goal of this section is to prove Theorem 3.10. Given a diagram of K and its algebra $\mathcal{A}(a_1, \dots, a_n)$, we will check that the stable tame isomorphism class of $\mathcal{A}$ is invariant under each of the three Legendrian Reidemeister moves (see Figure 7). As in Section 5, we will use an adaptation of Chekanov's original proof over $\mathbb{Z}/2$.

6.1. **Move I.** Let the algebras associated to the diagrams of K before and after move I be $\mathcal{A}(a, b, c, v_1, \dots, v_n; \partial)$ and $\mathcal{A}(a, b, c, v_1, \dots, v_n; \partial')$ respectively, where the crossings a, b, and c are indicated in Figure 8. In order to exhibit an elementary isomorphism between these two DGAs, we need some more notation. Figure 8 labels the twelve relevant quadrants by their orientation signs $\varepsilon_{i,a}, \varepsilon_{i,b}, \varepsilon_{i,c}$. Also, for either diagram in Figure 8, let $\gamma_a, \gamma_b, \gamma_c$ be the capping paths corresponding to the three crossings. As we approach the triple point intersection from either diagram, $\gamma_a - \gamma_b - \gamma_c$ limits to a cycle in $H_1(K)$; let k be the number of times it winds around K.

Define an elementary automorphism Φ on $\mathcal{A} = \mathcal{A}(a, b, c, v_1, \dots, v_n)$ by its action on the generators of $\mathcal{A}$:

$$\Phi(w) = \begin{cases} a - \varepsilon t^{-k} cb & \text{if } w = a \\ w & \text{otherwise,} \end{cases} \tag{6.1}$$

where $\varepsilon = \varepsilon_{4,a}\varepsilon_{4,b}\varepsilon_{1,c}$. We claim that Φ gives the desired tame isomorphism between the two DGAs.

We first note the following lemma, whose proof is similar to the proof of Lemma 3.4 and is omitted.

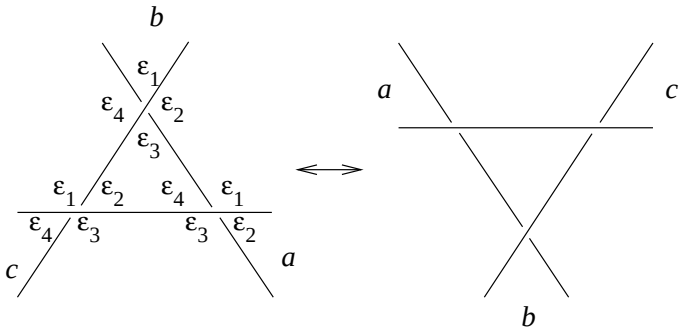

FIGURE 8. A labeling for the orientation signs $\varepsilon_{i,a}, \varepsilon_{i,b}, \varepsilon_{i,c}$ for the twelve relevant quadrants in move I. In the diagram, the subscript a, b, c is suppressed.

Lemma 6.1. *sgn* $a = (sgn\ b)(sgn\ c)$.

Similarly, it is not hard to show that Φ preserves the grading on $\mathcal{A}$.

It remains to show that Φ is a chain map, intertwining the actions of ∂ and ∂'. We demonstrate this on the generators of $\mathcal{A}$. It suffices to consider a and the generators whose differential has a term containing a, since move I does not change any of the other differentials (see [6]).

First consider a crossing v for which ∂v contains a. We may group the terms in ∂v and $\partial' v$ as follows:

(1) the terms in ∂v containing cb, and the corresponding terms in ∂v and $\partial' v$ replacing cb by a;
(2) the terms in $\partial' v$ containing cb, and the corresponding terms in ∂v and $\partial' v$ replacing cb by a;
(3) the remaining terms in ∂v and $\partial' v$, which are identical and do not contain a or cb.

For $i = 1, 2, 3$, denote by $\partial_i v$ and $\partial'_i v$ the contributions of these three groups to ∂v and $\partial' v$.

It is straightforward to check that $\partial_1 v$ is simply $\partial'_1 v$ with a replaced by $a + \varepsilon_{4,a}\varepsilon_{4,b}\varepsilon_{1,c} t^{-k} cb$, and so $\partial'_1 v = \Phi\partial_1 v$. Similarly, $\partial'_2 v$ is $\partial_2 v$ with a replaced by $a + \varepsilon_{2,a}\varepsilon_{2,b}\varepsilon_{3,c} t^{-k} cb$. By Lemmas 3.6 and 6.1, we have

$$\varepsilon_{2,a}\varepsilon_{4,a}\varepsilon_{2,b}\varepsilon_{4,b}\varepsilon_{1,c}\varepsilon_{3,c} = (-\text{sgn } a)(-\text{sgn } b)(-\text{sgn } c) = -1;$$

it follows that $\partial'_2 v = \Phi\partial_2 v$. Since we also have the trivial identity $\partial'_3 v = \Phi\partial_3 v$, we conclude that $\partial'\Phi v = \partial' v = \Phi\partial v$.

Finally, we consider ∂a and $\partial' a$. We may group the terms in ∂a and $\partial' a$ as follows:

(1) the disks in either ∂a or $\partial' a$ with positive corner in the quadrant labeled $\varepsilon_{1,a}$, which do not have an adjacent corner at b or c;
(2) the disks in either ∂a or $\partial' a$ with positive corner at $\varepsilon_{3,a}$ and no adjacent corner at b or c;
(3) the disks in ∂a (resp. $\partial' a$) with positive corner at $\varepsilon_{1,a}$ (resp. $\varepsilon_{3,a}$) and adjacent corner at b;
(4) the disks in ∂a (resp. $\partial' a$) with positive corner at $\varepsilon_{3,a}$ (resp. $\varepsilon_{1,a}$) and adjacent corner at c.

As before, let $\partial_i a$, $\partial'_i a$ be the contributions of these four groups to ∂a, $\partial' a$, for $i = 1, 2, 3, 4$.

Clearly $\partial_1 a = \partial'_1 a$ and $\partial_2 a = \partial'_2 a$. On the other hand, gluing the middle triangle to any disk in $\partial_3 a$ or $\partial'_3 a$ gives a disk with positive corner at c, and any disk in $\partial c = \partial' c$ is obtained this way. The sign and power-of-t difference between terms in $\partial_3 a$ and the corresponding terms in $\partial' c$ is $\varepsilon_{1,a}\varepsilon_{2,b}\varepsilon_{2,c}t^{-k} = -\varepsilon t^{-k}$ by Lemma 3.6, while the difference between terms in $\partial'_3 a$ and the corresponding terms in $\partial' c$ is $\varepsilon_{3,a}\varepsilon_{4,b}\varepsilon_{4,c}t^{-k} = \varepsilon t^{-k}$; hence $\partial'_3 a - \partial_3 a = \varepsilon t^{-k}(\partial' c)b$. Similarly, $\partial'_4 a - \partial_4 a = (\text{sgn } c)\varepsilon t^{-k} c(\partial' b)$. We conclude that

$$\partial' a - \partial a = \varepsilon t^{-k}((\partial' c)b + (\text{sgn } c)c(\partial' b)) = \varepsilon t^{-k}\partial'(cb). \tag{6.2}$$

Hence $\Phi\partial a = \partial'\Phi a$, as desired.

6.2. **Move II.** Let the algebras associated to the diagrams of K before and after move II be the same as for move I. In this case, we claim that $\partial = \partial'$. The fact that there are no new disks, unlike in move I, is derived from the following corollary of Stokes' theorem:

Lemma 6.2 (Chekanov)**.** *Let $u : (D^2_*, S^1_*) \to (\mathbb{C}, K)$ be a holomorphic disk with positive punctures $t_1, \dots, t_n$ and negative punctures $\tau_1, \dots, \tau_m$. Denote the height of the crossing a by $h(a)$. Then*

$$\sum_1^n h(u(t_i)) - \sum_1^m h(u(\tau_i)) = \int_{D^2_*} u^*(dx \wedge dy) > 0. \tag{6.3}$$

See [6] for a detailed account.[1] The signs and powers of t do not change since all disks cover exactly the same quadrants at the crossings before and after the move. Hence $\partial = \partial'$.

6.3. **Move III.** Let a and b denote the two new crossings produced by move III, as labeled in Figure 9. We may then write the algebras associated to the diagrams of K before and after move III as

$$\mathcal{A} = \mathcal{A}(a, b, a_1, \dots, a_n, b_1, \dots, b_m; \partial)$$
$$\mathcal{A}' = \mathcal{A}(a_1 \dots, a_n, b_1, \dots, b_m; \partial').$$

Furthermore, suppose that the other crossings are ordered by height:

$$h(a_n) \geq \cdots \geq h(a_1) \geq h(a) > h(b) \geq h(b_1) \geq \cdots \geq h(b_m). \tag{6.4}$$

The orientation signs $\varepsilon_a, \varepsilon'_a, \varepsilon_b, \varepsilon'_b$ for four relevant quadrants have been labeled in Figure 9. Note that, due to our choice of capping paths in Section 3.1, γ_a and γ_b limit to the same path as a and b approach each other; hence the term in ∂a corresponding to the 2-gon with corners at a and b is $\varepsilon_a\varepsilon_b b$. Lemma 6.2 then tells us that $\partial a = \varepsilon_a\varepsilon_b b + \varepsilon'_a v$, where v is a sum of terms in the b_i and t. Note for future reference that Lemma 3.6 implies that $\varepsilon_a\varepsilon'_a = -\text{sgn } a$ and $\varepsilon_b\varepsilon'_b = -\text{sgn } b$; also, since ∂ lowers degree by 1, we have $(\text{sgn } a)(\text{sgn } b) = -1$.

We now define a grading-preserving elementary isomorphism $\Phi_0 : \mathcal{A} \to S_{|a|}(\mathcal{A}')$ by its action on generators:

$$\Phi_0(w) = \begin{cases} e_1 & w = a \\ \varepsilon_a\varepsilon_b e_2 + \varepsilon'_b v & w = b \\ w & \text{otherwise.} \end{cases} \tag{6.5}$$

Although Φ_0 is not a chain map on $\mathcal{A}$, it is not far off, as illustrated by the two lemmas below. Define $\mathcal{A}_i = S_{|a|}(\mathcal{A}(a_1, \dots, a_i, b_1, \dots, b_m))$, and let $\tau : S(\mathcal{A}) \to \mathcal{A}$ be the obvious projection map.

[1] Chekanov uses "move IIIa" to denote our move II.

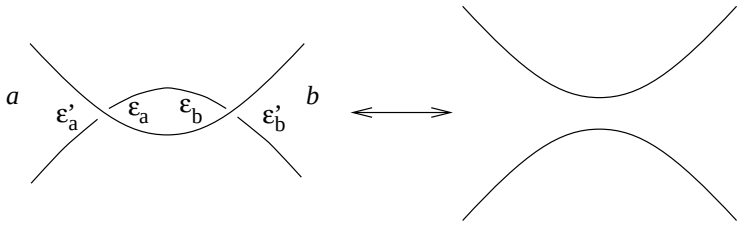

FIGURE 9. A labeling for the crossings in move III; $\varepsilon_a, \varepsilon'_a, \varepsilon_b, \varepsilon'_b$ are orientation signs at crossings a and b.

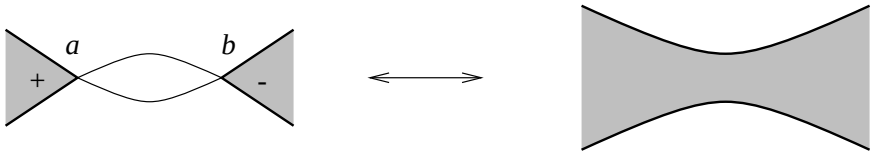

FIGURE 10. Piecing together two disks from ∂ to get a disk in ∂'. The signs are Reeb signs, and the crossing a_i is schematically located off to the right in both figures.

Lemma 6.3. $\Phi_0|_{\mathcal{A}_0}$ *is a chain map.*

Proof. We prove this on generators of $\mathcal{A}_0$. There is nothing to prove for the b_i since, by Lemma 6.2, ∂b_i contains only terms involving b_j with $j > i$. On the other hand, direct computation shows that $\Phi_0 \partial a = e_2 = \partial' \Phi_0 a$ and $\Phi_0 \partial b = \partial b = \partial \Phi_0 b$. □

Lemma 6.4. $\tau \circ \partial' \circ \Phi_0 = \tau \circ \Phi_0 \circ \partial$.

Proof. By Lemma 6.3, it suffices to prove equality on the generators a_i. Let W_1 denote the sum of the terms which appear in both ∂a_i and $\partial' a_i$; let W_2 denote the sum of the terms in ∂a_i involving b; and write $\partial a_i = W_1 + W_2 + W_3$ and $\partial' a_i = W_1 + W_4$.

The terms in W_1 do not contain a or b, and so $\Phi_0 W_1 = W_1$. The terms in W_3 must involve a; since $\Phi_0(a) = e_1$, we have $\tau \Phi_0 W_3 = 0$.

Now consider the terms in W_4; these arise from disks of the type shown on the right in Figure 10. There is a one-to-one correspondence between these disks and pairs of disks in ∂, one with positive corner at a_i and a negative corner at b, and one with positive corner at a. Thus W_4 is the result of taking W_2 and replacing every occurrence of b by $\varepsilon'_a \varepsilon'_b (\partial a - \varepsilon_a \varepsilon_b b) = \varepsilon'_b v$; in other words, $W_4 = \tau \Phi_0 W_2$.

We conclude that

$$\tau \partial' \Phi_0 a_i = \partial' a_i = W_1 + W_4 = W_1 + \tau \Phi_0 W_2 = \tau \Phi_0 \partial a_i, \tag{6.6}$$

as desired. □

Using Lemmas 6.3 and 6.4, we bootstrap Φ_0 up to a map Φ_n which is the desired chain map on $\mathcal{A}$, by inductively defining maps Φ_i which are chain maps when restricted to $\mathcal{A}_i$. We define Φ_i along with elementary automorphisms g_i of $S(\mathcal{A})$ as follows. Let $H : S(\mathcal{A}') \to S(\mathcal{A}')$ be the map from the proof of Corollary 3.11. Define g_i to fix all generators except a_i, and

$$g_i(a_i) = a_i + H(\partial' a_i - \Phi_{i-1} \partial a_i); \tag{6.7}$$

then define $\Phi_i = g_i \Phi_{i-1}$.

We collect several facts that we will need. Recall equation (3.8) from the proof of Corollary 3.11, namely:

$$\tau - Id = \partial' H + H\partial'.$$

Also, since $\tau H = 0$, we have $\tau g_i = \tau$ for all i, and hence $\tau \Phi_i = \tau \Phi_0$ for all i. Finally, note that, because the a_j are ordered by height, $\partial a_i \in \mathcal{A}_{i-1}$.

Now assume that $\Phi_{i-1}|_{\mathcal{A}_{i-1}}$ is a chain map, i.e., that $\partial' \Phi_{i-1} = \Phi_{i-1}\partial$ on $\mathcal{A}_{i-1}$; we show that $\Phi_i|_{\mathcal{A}_i}$ is a chain map. We can now calculate, at one point using Lemma 6.4:

$$\begin{aligned}
\Phi_{i-1}\partial a_i &= \tau\Phi_{i-1}\partial a_i - \partial' H \Phi_{i-1}\partial a_i - H\partial'\Phi_{i-1}\partial a_i \\
&= \tau\Phi_0\partial a_i - \partial' H \Phi_{i-1}\partial a_i - H\Phi_{i-1}\partial^2 a_i \\
&= \tau\partial'\Phi_0 a_i - \partial' H \Phi_{i-1}\partial a_i \\
&= (Id + \partial' H + H\partial')\partial' a_i - \partial' H \Phi_{i-1}\partial a_i \\
&= \partial'(a_i + H\partial' a_i - H\Phi_{i-1}\partial a_i) \\
&= \partial' g_i(a_i).
\end{aligned} \tag{6.8}$$

Since $\Phi_{i-1}\partial a_i \in \mathcal{A}_{i-1}$, it follows that $\Phi_i \partial a_i = \partial' g_i(a_i) = \partial' \Phi_i a_i$. On the other hand, the induction hypothesis implies that $\Phi_i \partial = \partial' \Phi_i$ on $\mathcal{A}_{i-1}$. Hence Φ_i is a chain map on $\mathcal{A}_i$, completing the induction.

This concludes the proof of Theorem 3.10. □

Part II
A Geometric Framework

In this part of the paper, we show that the combinatorial theory developed in the previous sections fits into a much richer geometric framework. In Section 7, we show that our combinatorial theory is a faithful translation of Eliashberg and Hofer's definition of (relative) contact homology. Their theory is much more general and provides invariants for Legendrian submanifolds in any contact manifold. However, it is hard to make computations in their setup, so it is helpful to know that the (easy) combinatorial definition of the contact homology for Legendrian knots in $\mathbb{R}^3$ is equivalent to their definition. Moreover, having Eliashberg and Hofer's geometric ideas in mind makes some of the combinatorial proofs more transparent. Finally, in Section 8 we describe "coherent orientations" in contact homology and show that, when translated into our combinatorial framework, they yield the sign conventions described in Part I.

7. Relative Contact Homology

The goal of this section is to sketch a relative version of Eliashberg and Hofer's contact homology theory. Our presentation is similar to that of [8, Section 2.7], in which relative contact homology is set in the more general context of "symplectic field theory". We will then specialize to the case of Legendrian knots in the standard contact structure on $\mathbb{R}^3$ and will show how to project the general theory into the xy plane. There the objects in the definition of contact homology can be seen to be combinatorial in nature. Note that the analytic details of the general theory have yet to be completed. When the general theory is worked out, our translation shows that computations in the combinatorial setting are also computations in the general theory.

7.1. **The General Case.** Let us begin by setting up some notation. Let $(M;\xi)$ be a contact 3-manifold with contact form α. Let K be a Legendrian knot in M. For simplicity of presentation, we consider only the case where $H_1(M) = 0$ and $H_2(M) = 0$. Thus, we may identify $H_2(M,K)$ and $H_1(K)$ via the standard boundary homomorphism. Further, a choice of orientation on K induces an identification of $H_1(K)$ with $\mathbb{Z}$. Let X_α be the Reeb vector field of α. A segment of a flow line for X_α starting and ending on K is called a **Reeb chord** for K.

Definition 7.1. Let $\mathcal{A}$ be the free associative graded unital algebra over the group ring $\mathbb{Z}[H_2(M,K)] = \mathbb{Z}[H_1(K)]$ generated by the Reeb chords in $(M,K;\alpha)$. The generators of $\mathcal{A}$ are graded by their Conley-Zehnder indices (see below). The generator t of $\mathbb{Z}[H_1(K)]$ is graded by $2\,r(K)$.

To define the Conley-Zehnder index of a Reeb chord $a(t)$, we must fix a "capping path" γ_a inside K that connects $a(1)$ to $a(0)$. Next, we choose a surface F_a with $\partial F_a = a \cup \gamma_a$ and a trivialization of ξ over F_a. Let E be the sub-bundle of ξ over $a \cup \gamma_a$ defined by:

$$\begin{aligned} E|_{\gamma_a(t)} &= T_{\gamma_a(t)}K \\ E|_{a(t)} &= D\Phi_\alpha(t)\cdot T_{a(0)}K, \end{aligned} \tag{7.1}$$

where Φ_α is the flow of X_α. Using the trivialization, the sub-bundle E may be viewed as a path of Lagrangian subspaces in a fixed symplectic vector space. Let $CZ(a)$ be the Conley-Zehnder index of this path, as defined in [18].

While the Conley-Zehnder index is independent of the choices of F_a and the trivialization of ξ over F_a, it does depend on the choice of capping path γ_a. Suppose that $\tilde{\gamma_a}$ is another such choice. Since the paths γ_a and $\tilde{\gamma_a}$ have the same starting and ending points, they differ up to homotopy by a path γ_n that winds n times around the knot K. We have:

$$\begin{aligned} CZ(\gamma) &= \mu(\gamma_n) + CZ(\tilde{\gamma}) \\ &= n\,\mu(\gamma_1) + CZ(\tilde{\gamma}). \end{aligned} \tag{7.2}$$

Here, μ is the Maslov index of a loop of Lagrangian subspaces. As we saw in Section 3.1, we can get a true $\mathbb{Z}$ grading on A by making the choice of capping path explicit in the algebraic structure.

To define a differential ∂ on $\mathcal{A}$, we must consider the symplectization $(M\times\mathbb{R}, \omega = d(e^\tau\alpha))$ of (M,ξ), and fix an almost complex structure J which is compatible with the symplectic form (*i.e.* $\omega(v,Jv) > 0$ for $v \neq 0$), and which, in addition, satisfies:

$$\begin{aligned} J(\partial_\tau) &= X_\alpha \\ J(\xi) &= \xi. \end{aligned} \tag{7.3}$$

Now the differential ∂ on $\mathcal{A}$ is defined by counting certain rigid J-holomorphic curves in the symplectization $(M\times\mathbb{R}, d(e^\tau\alpha))$.

The J-holomorphic curves that we count are maps

$$f : (D^2_*, \partial D^2_*) \to (M\times\mathbb{R}, K\times\mathbb{R}) \tag{7.4}$$

where $D^2_* = D^2 \setminus \{x, y_1, \ldots, y_n\}$ and $\{x, y_1, \ldots, y_n\}$ lies in ∂D^2. Let f_M be the projection of f to M and let $f_\mathbb{R}$ be the projection of f to $\mathbb{R}$. We want these disks to have boundary in the Lagrangian submanifold $K\times\mathbb{R}$ and to satisfy some asymptotic conditions near the punctures. Note that a neighborhood of a boundary puncture $x \in \partial D^2$ is conformally equivalent to the strip $(0,\infty)\times[0,1]$ with coordinates (s,t) such that approaching ∞ in the strip is equivalent to approaching x in the disk.

Definition 7.2. We say that f, parametrized as above near a boundary puncture x, **tends asymptotically to a Reeb strip** over the Reeb chord $a(t)$ at $\pm\infty$, if:

$$\begin{aligned} \lim_{s\to\infty} f_{\mathbb{R}}(s,t) &= \pm\infty \\ \lim_{s\to\infty} f_M(s,t) &= a(t). \end{aligned}$$

See [1] for convergence results for J-holomorphic curves near boundary punctures. We are now ready to define the moduli spaces involved in the differential.

Definition 7.3. $\mathcal{M}^A(a; b_1, \dots, b_n)$, the **moduli space of J-holomorphic disks** realizing the homology class $A \in H_2(M, K) \cong H_1(K)$, and with a positive puncture at the Reeb chord a and (cyclically ordered) negative punctures at the Reeb chords $b_1, \dots, b_n$, consists of all proper J-holomorphic maps f as in equation (7.4), that satisfy the following conditions:

(1) The map f has finite energy:

$$\int_{D^2_*} f^* d\alpha < \infty. \tag{7.5}$$

(2) The cycle $f_M(\partial D^2_*) \cup \gamma_a \cup -\gamma_{b_1} \cup \cdots \cup -\gamma_{b_n}$ represents the homology class A.
(3) Near x, f tends asymptotically to a Reeb strip over a at $+\infty$.
(4) Near y_j, f tends asymptotically to a Reeb strip over b_j at $-\infty$.

Two maps f and g in $\mathcal{M}^A(a; b_1, \dots, b_n)$ are equivalent if there is a conformal map $\phi : D^2_* \to D^2_*$ such that $f = g \circ \phi$.

Since J is invariant under translation in the "vertical" τ direction, every J-holomorphic disk is part of a vertically invariant family. To alleviate confusion, we will denote the dimension of $\mathcal{M}^A$ by $k+1$, where the 1 indicates dimension in the vertically invariant τ direction.

The local structure of the moduli space $\mathcal{M}^A(a; b_1, \dots, b_n)$ near a map f may be analyzed using the Implicit Function Theorem. Consider the linearization of the $\bar\partial$ operator at f:

$$D_f\bar\partial : \Omega^0(f^*T(M \times \mathbb{R})) \to \Omega^{0,1}(f^*T(M \times \mathbb{R})).$$

Assuming sufficient genericity of the data and a suitable Sobolev (or Hölder) setup (see [14], for example), this map is surjective and Fredholm. The Implicit Function Theorem gives a local parametrization of $\mathcal{M}^A(a; b_1, \dots, b_n)$ whose domain is a neighborhood of zero in the kernel of $D_f\bar\partial$. The dimension of the moduli space is given by:

Proposition 7.4 ([5])**.**

$$\dim \mathcal{M}^A(a; b_1, \dots, b_n) = CZ(a) - \sum CZ(b_j) + 2r(K) \cdot A.$$

Finally, we define a differential on $\mathcal{A}$ using all $(0+1)$-dimensional moduli spaces:

Definition 7.5. Let $a, b_1, \dots, b_n$ be Reeb chords. Define:

$$\partial(a) = \sum_{\dim(\mathcal{M}^A(a;b_1,\dots,b_n))=0+1} (\#\mathcal{M}/\mathbb{R}) t^A b_1 \cdots b_n.$$

Here, the number of points in $\mathcal{M}$ is counted with sign using an orientation on $\mathcal{M}$ described in Section 8.

In general, we expect that ∂ makes $\mathcal{A}$ into a differential graded algebra whose homology is an invariant of the Legendrian knot and the contact structure (see [8]). The remainder of this section proves the invariance of $(\mathcal{A}, \partial)$ for Legendrian knots in $\mathbb{R}^3$ with the fixed form α_0 by translating everything into the combinatorial setting of Part I.

7.2. **A Two-Dimensional Projection.** We now specialize to the case of an oriented Legendrian knot K in $(\mathbb{R}^3, \alpha_0)$. The first step in translating the general relative contact homology theory into Chekanov's combinatorial DGA is to project all of the objects involved in the definition of $\mathcal{A}$ into the xy plane. Suppose that K that admits a generic projection to the xy plane.

Since the Reeb field of α_0 is ∂_z, the crossings of the diagram of K correspond to the Reeb chords of $(\mathbb{R}^3, K, \alpha_0)$. We choose capping paths and grade the crossings by their Conley-Zehnder indices. Note that the contact planes ξ_0 may be globally trivialized by ∂_x and $\partial_y - x\,\partial_z$. In the projection, these are just the standard coordinate vector fields and hence, modulo the correction at the end of the path, the Conley-Zehnder index is just twice the rotation number of the path with respect to the standard trivialization of $T\mathbb{R}^2$.

Next, we describe an explicit J for the symplectization $(\mathbb{R}^3 \times \mathbb{R}, d(e^\tau \alpha_0))$. Recall that the compatible almost complex structure described in Section 7.1 must satisfy equation (7.3). Since the Reeb field is ∂_z, the following J works:

$$\begin{aligned} J(\partial_x) &= \partial_y - x\partial_z \\ J(\partial_y) &= -x\partial_\tau - \partial_x \\ J(\partial_z) &= -\partial_\tau \\ J(\partial_\tau) &= \partial_z. \end{aligned} \tag{7.6}$$

Write a map $f : D^2_* \to \mathbb{R}^3 \times \mathbb{R}$ as

$$f(u,v) = (x(u,v), y(u,v), z(u,v), \tau(u,v)). \tag{7.7}$$

Using the J in (7.6), we can write down the $\bar{\partial}_J$ equations for f as follows:

$$\begin{aligned} \partial_u x - \partial_v y &= 0 \\ \partial_u y + \partial_v x &= 0 \\ \partial_u \tau - \partial_v z &= x\partial_v y \\ \partial_u z + \partial_v \tau &= x\partial_u x. \end{aligned} \tag{7.8}$$

Thus, the xy projections of J-holomorphic maps of D^2_* are actually holomorphic as maps to $\mathbb{C}$ (i.e. the xy-plane endowed with the standard complex structure). It follows that every moduli space of J-holomorphic disks projects to a family of holomorphic maps

$$f : (D^2_*, \partial D^2_*) \to (\mathbb{C}, \pi_{xy}(K)). \tag{7.9}$$

The conditions on the J-holomorphic disks in $\mathcal{M}^A(a; b_1, \ldots, b_k)$ translate to the following restrictions on the maps f:

(1) The homology class $\left[(\pi_{xy}|_K)^{-1}\left(\mathrm{Im}(f|_{\partial D^2}) \cup \gamma_a \cup -\gamma_{b_1} \cup \cdots \cup -\gamma_{b_n}\right)\right]$ coincides with A.
(2) The map f sends the boundary punctures to the crossings of the diagram of K. At a boundary puncture, the map f covers either one or three quadrants, with the majority of the quadrants positive at the crossing a and negative at the crossings b_i.

Definition 7.6. The space of maps $\Delta^A_h(a; b_1, \ldots, b_n)$ consists of all holomorphic maps f as in equation (7.9) that satisfy conditions 1 and 2 above.

We consider two maps f and g in Δ^A_h to be equivalent if there is a conformal map $\phi : D^2_* \to D^2_*$ such that $f = g \circ \phi$.

The spaces $\Delta_h^A(a; b_1, \dots, b_n)$ are clearly subsets of the combinatorially defined spaces $\Delta^A(a; b_1, \dots, b_n)$ introduced in Definition 3.3. We use the spaces Δ_h^A as a convenient intermediate step in showing the equivalence between $\mathcal{M}^A(a; b_1, \dots, b_n)$ and $\Delta^A(a; b_1, \dots, b_n)$.

Define a projection map p by:

$$\begin{aligned} \mathcal{M}^A(a; b_1, \dots, b_n)/\mathbb{R} &\to \Delta_h^A(a; b_1, \dots, b_n) \\ f &\mapsto \pi_{xy} \circ f. \end{aligned} \tag{7.10}$$

Here the $\mathbb{R}$-action is vertical translation.

Theorem 7.7 (Translation Theorem)**.** *The following three spaces are homeomorphic:*

(1) $\mathcal{M}^A(a; b_1, \dots, b_n)/\mathbb{R}$
(2) $\Delta_h^A(a; b_1, \dots, b_n)$
(3) $\Delta^A(a; b_1, \dots, b_n)$

The projection p gives an explicit homeomorphism between the first two. The inclusion of Δ_h^A into Δ^A gives the homeomorphism between the last two.

Note that this implies:

$$\dim \Delta^A(a; b_1, \dots, b_n) = \dim \mathcal{M}^A(a; b_1, \dots, b_n) - 1. \tag{7.11}$$

We will postpone the proof until the end of the section. Since the theorem tells us that p is a homeomorphism, any system of coordinates we find on the spaces Δ_h^A can be lifted to coordinates on the moduli spaces $\mathcal{M}^A$ (along with a coordinate that parametrizes the vertical translations in $\mathcal{M}^A$). As it turns out, we can use classical complex analysis to coordinatize Δ_h^A.

Proposition 7.8. *The space $\Delta_h^A(a; b_1, \dots, b_n)$ has local coordinates given by the images of n interior branch points and m branch points on the boundary. Thus,*

$$2n + m = \dim \Delta_h^A. \tag{7.12}$$

Proof. Let $f \in \Delta_h^A$. Construct a Riemann surface S for the inverse of f by analytic continuation. Think of S as a branched cover over the image of f. Let $\tilde{f}$ be the lifting of f to a map from D_*^2 to S. Since the inverse of f is single-valued on S, $\tilde{f}$ must be an homeomorphism. Using this construction, we must prove first that f is the unique map in Δ_h^A with a given configuration of branch points in the image, and second that any small variation of the images of the branch points can be accomplished inside Δ_h^A.

For the first part, suppose that g is an element of Δ_h^A whose branch points have the same images as those of f. Then g lifts as a biholomorphism to $\tilde{g} : D_*^2 \to S$. The map $\tilde{g} \circ \tilde{f}^{-1}$ is an automorphism of the disk, and hence $\tilde{g}$ and $\tilde{f}$ differ only by a reparametrization. Projecting down to $\mathbb{C}$, we see that f and g differ only by a reparametrization, or in other words, $f \sim g$ in Δ_h^A.

For the second part, let S' be the Riemann surface obtained by perturbing the image of the branch locus of S in $\mathbb{C}$. Note that S' projects to a different region in $\mathbb{C}$ when a boundary branch point is perturbed along the diagram of K. Since small perturbations of the image of the branch locus do not change the topology of S, the Uniformization Theorem provides a biholomorphism $g : D^2 \to S'$ that projects to an element of Δ_h^A.

Finally, each interior branch point has two degrees of freedom, whereas a boundary branch point contributes but one; the formula (7.12) follows. □

We end this section with a proof of Theorem 7.7.

Proof of Theorem 7.7. We prove this theorem in two steps. We show first that $\Delta_h^A = \Delta^A$, and then that the projection from $\mathcal{M}^A/\mathbb{R}$ to Δ_h^A is a homeomorphism.

To prove $\Delta_h^A = \Delta^A$, we clearly need only to show that $\Delta^A \subset \Delta_h^A$. To this end, let $f : D_*^2 \to \mathbb{C}$ be an immersion satisfying the conditions for Δ^A. Use f to pull back the complex structure from $\mathbb{C}$. Then the Riemann Mapping Theorem provides a conformal equivalence g between the new complex structure and the standard structure on the interior of D^2. Hence $f \circ g$ is holomorphic on the interior of D_*^2. That f lies in Δ_h^A now follows from the proof of Proposition 7.8 and the fact that holomorphic maps preserve orientation.

We are left to show that $p : \mathcal{M}^A/\mathbb{R} \to \Delta_h^A$ is a homeomorphism. It is clear from the discussion above that the image of p lies in Δ_h^A. The interesting part of the proof lies in the construction of an inverse q to p that lifts maps in Δ_h^A to $\mathcal{M}^A$. To do this, note that a few simple manipulations of the $\bar{\partial}_J$ equations (7.8) give, for $g = (x, y, z, \tau) \in \mathcal{M}^A$:

Lemma 7.9. *$z(u, v)$ is harmonic.*

Thus, given $f = (x, y) \in \Delta_h^A$, we define $z(u, v)$ by solving the Dirichlet problem with a (discontinuous) boundary condition which may be formulated as follows: suppose that $(u, v) \in \partial D_*^2$. By assumption, $(x(u, v), y(u, v))$ lies in the diagram of K. Away from the crossings, let $z(u, v)$ be the z coordinate of the knot K that lies above $(x(u, v), y(u, v))$. This defines the boundary condition $z(u, v)$ uniquely on ∂D_*^2.

Once we have determined $z(u, v)$, a similar manipulation of the $\bar{\partial}_J$ equations (7.8) yields:

Lemma 7.10. *$\partial_{uv}\tau = \partial_{vu}\tau$.*

Combined with the Poincaré Lemma, Lemma 7.10 tells us that we can find a $\tau(u, v)$ (unique up to an additive constant) so that $q(f) = (x, y, z, \tau)$ lifts f and solves the $\bar{\partial}_J$ equations on the interior of D^2. In fact, the solutions extend continuously to the boundary away from the punctures $x, y_1, \ldots, y_n$.

The lift $q(f)$ clearly satisfies condition 2 of the definition of $\mathcal{M}^A(a; b_1, \ldots, b_n)$. The first and last two conditions, namely that of finite energy and of asymptotic approach to Reeb strips at the punctures, need proof. We tackle the last condition first.

We begin by describing a local model for the lifting $q(f)$ near a positive puncture in the special case where the crossing that is the image of $f(x)$ is bounded by the x and y axes. Further, suppose that the lift $\tilde{L}_0$ of the x axis has constant z coordinate 0 and that the lift $\tilde{L}_1$ of the y axis has constant z coordinate $\pi/2$. In the xy plane, the exponential map takes the strip $\Sigma = \mathbb{R}_+ \times i[0, \pi/2]$ to the lower right-hand quadrant. Consider the following lifting $q(f)$ of f:

$$\begin{aligned} \Sigma &\to \mathbb{R}^3 \times \mathbb{R} \\ u + iv &\mapsto \left(e^{-u}\cos(v), -e^{-u}\sin(v), v, u + \frac{e^{-2u}}{2}\cos^2(v) \right). \end{aligned} \tag{7.13}$$

It is straightforward to check that this map is J-holomorphic and tends asymptotically to the Reeb chord over the origin as u goes to ∞.

It is not hard to generalize this model to the case where $\tilde{L}_0$ and $\tilde{L}_1$ are arbitrary straight lines whose projections L_0 and L_1 pass through the origin. Note that, in this case, the original map f is $f(u + iv) = c_0 e^{-\nu(u+iv)}$, where $c_0 \in L_0$, $c_0 e^{i\frac{\pi}{2}\nu_0} \in L_1$, $0 < \nu_0 < 1$, and $\nu = k - \nu_0$ for some integer k.

A theorem of Robbin and Salamon shows that every positive puncture is $O(e^{-Ks})$-close to a straight-line model in the xy-plane:

Theorem 7.11 (Robbin and Salamon [19]). *Let L_0 and L_1 be curves in $\mathbb{C}$ that pass through the origin. Let $f : \Sigma \to \mathbb{C}$ be a holomorphic map that satisfies:*

(1) $f(\mathbb{R}_+ \times \{\frac{\pi j}{2}\}) \subset L_j$ *for* $j = 0, 1$.
(2) $\lim_{u\to\infty} f(u, v) = \lim_{u\to\infty} \partial_u f(u, v) = 0$ *uniformly in* v.

Then there exist constants $c_0 \in \mathbb{C}^*$, $\nu \in \mathbb{R}_+$, and $\delta \in \mathbb{R}_+$ such that

$$f(u, v) = c_0 e^{-\nu(u+iv)} + O(e^{-(\nu+\delta)u}),$$

with $c_0 \in T_0 L_0$, $c_0 e^{i\frac{\pi}{2}\nu_0} \in T_0 L_1$, $0 < \nu_0 < 1$, and $\nu = k - \nu_0$ for some integer k.

Given a crossing with curves $\tilde{L}_0$ and $\tilde{L}_1$, let $f : \Sigma \to \mathbb{C}$ be a holomorphic curve that satisfies the hypotheses of Theorem 7.11. Let f_0 be a straight-line solution with respect to the lines $T_0\tilde{L}_0$ and $T_0\tilde{L}_1$. The theorem asserts that these two solutions differ by $O(e^{-(\nu+\delta)u})$. Further, a simple calculation using the fact that the z coordinates of $\tilde{L}_j$ are determined from their xy coordinates shows that the boundary conditions for the Dirichlet problem differ by $O(e^{-(\nu+\delta)u})$. By the maximum principle, the z liftings of f and f_0 differ by at most $O(e^{-(\nu+\delta)s})$. Furthermore, by explicitly writing out the formula for the liftings to the τ coordinate that come from the proof of the Poincaré Lemma (see [4], for example), we see that the difference there is $O(ue^{-(\nu+\delta)u})$.

Thus, on the strip Σ, the lifting of the straight-line model is exponentially close to the lifting of the general case. Since the straight-line case tends asymptotically to a Reeb chord, so must the general case.

Finally, we have to show that $q(f)$ has finite energy. Let S_0 be a small half-disk around the puncture x in the disk D^2_*. Similarly, for each i, let S_i be a half-disk around y_i. Let Γ be the boundary of $D^2 \setminus \cup S_i$. Stokes' Theorem gives:

$$\int_{D^2\setminus\cup S_i} q(f)^* d\alpha = \int_\Gamma q(f)^*\alpha. \tag{7.14}$$

As the S_i get smaller, Γ approaches ∂D^2_* and so, using the straight-line model and Theorem 7.11, we have:

$$\int_\Gamma q(f)^*\alpha \to \int_a \alpha - \sum_i \int_{b_i} \alpha < \infty. \tag{7.15}$$

This completes the proof that the inverse map $q : \Delta^A_h \to \mathcal{M}^A/\mathbb{R}$ is well-defined. Using the same methods as for the characterization of the asymptotic behavior of $q(f)$, it is clear that q is a continuous inverse to p. The theorem follows. □

Remark. Theorem 7.7 and Proposition 7.8 apply to the more general setting in which disks with multiple positive boundary punctures are present. Such disks must be understood when trying to generalize contact homology to symplectic field theory.

8. Coherent Orientations

In this section we describe Floer and Hofer's idea of coherent orientations [12] in the context of contact homology [8]. This allows the signed count of points in $\mathcal{M}^A$ used in the definition of ∂. In Section 8.2, we will then translate these orientations on $\mathcal{M}^A$ to orientations on Δ^A using Theorem 7.7. We show in Section 8.3 that these orientations yield the sign conventions used in Part I.

8.1. **Geometric Ideas.** The geometric idea behind orienting the moduli spaces $\mathcal{M}^A$ discussed in Section 7 comes from Floer and Hofer's **coherent orientations**. In [12], they detailed a program for orienting the moduli spaces relevant to Floer homology for periodic orbits of Hamiltonian systems, in which the moduli spaces involve maps of infinite cylinders that limit to periodic orbits at each end. In [8], Eliashberg, Givental, and Hofer generalized and refined the coherent orientation idea to the setting of symplectic field theory, of which contact homology is a special case. In this section, we will adapt their ideas to the relative setting in $\mathbb{R}^3$.

This first step in the coherent orientation program is to consider the operators involved in the definition of the moduli space $\mathcal{M}^A(a; b_1, \ldots, b_k)$ rather than just the moduli space itself. Recall that $\mathcal{M}^A(a; b_1, \ldots, b_k)$ is the space of J-holomorphic maps from the boundary-punctured disk $D^2_* = D^2 \setminus \{x, y_1, \ldots, y_n\}$ to $\mathbb{R}^3 \times \mathbb{R}$ that send the boundary of the punctured disk to $K \times \mathbb{R}$ and tend asymptotically to the Reeb chords $a, b_1, \ldots, b_n$ at the punctures. Let $f \in \mathcal{M}^A(a; b_1, \ldots, b_k)$. The linearized operator $D_f\bar{\partial}_J$ on $f^*T(\mathbb{R}^3 \times \mathbb{R})$ is Fredholm in the proper analytic setup. When $D_f\bar{\partial}_J$ is surjective, the Implicit Function Theorem gives a local coordinate system on $\mathcal{M}^A(a; b_1, \ldots, b_k)$. Thus, in order to orient $\mathcal{M}^A(a; b_1, \ldots, b_k)$, it suffices to orient the kernel bundle of the operators $D_f\bar{\partial}_J$ for $f \in \mathcal{M}^A$.

Instead of doing this, Floer and Hofer's idea was to expand the set of operators under consideration beyond the $D_f\bar{\partial}_J$ operators to the space of **Cauchy-Riemann-type** operators that share the boundary conditions and asymptotic behavior with the "honest" operators that come from the moduli space. In fact, their program orients Cauchy-Riemann-type operators on all complex bundles over all closed Riemann surfaces.

In order to define Cauchy-Riemann-type operators in the relative case, we introduce holomorphic coordinates $(0, \infty) \times i[0, \pi/2]$ near each puncture on the boundary of a Riemann surface S_* with boundary. Compactify each puncture y_k with an interval I_k to get $(0, \infty] \times i[0, \pi/2]$. Call the compactified Riemann surface $\hat{S}$.

Definition 8.1 (Compare with [8])**.** A **smooth complex vector bundle** E **over** S_* is a smooth complex bundle over $\hat{S}$ together with Hermitian trivializations $\Phi_k : E|_{I_k} \to [0, \pi/2] \times \mathbb{C}^n$ and a real sub-bundle E^∂ over ∂S_*. An isomorphism between bundles must respect the Hermitian trivializations over I_k and the real sub-bundle E^∂.

In this setup, the appropriate sections of E to consider are those which map the boundary of S_* to the real sub-bundle E^∂. In fact, we want to consider sections in the Sobolev space $H^{1,2}_{loc}(S_*, E)$ that, in addition, lie in $H^{1,2}((0, \infty] \times i[0, \pi/2], E)$ with respect to local "strip" coordinates near each puncture. We call the space of such sections $H^{1,2}(E)$; a similar definition applies to L^2 sections.

Given a bundle E, define X_E to be the bundle whose fiber over z consists of (i, J)-anti-linear maps $\varphi : T_z\hat{S} \to E_z$. We want to consider operators $L : H^{1,2}(E) \to L^2(X_E)$ which have the form:

$$(Lh) \cdot X = \nabla_X h + J\nabla_{iX} h + A(h) \cdot X. \tag{8.1}$$

Here, h is a section in $H^{1,2}(E)$, X is a vector field on S, and A is a section of $\mathrm{Hom}_{\mathbb{R}}(E, X_E)$. The operators L must satisfy an asymptotic condition near the punctures. Namely, in local strip coordinates $(s, t) \in (0, \infty] \times i[0, \pi/2]$, L must take the form:

$$(Lh) \cdot \partial_s = \partial_s h - A(s, t) \cdot h. \tag{8.2}$$

Furthermore, $A(s,t) \to -i\partial_t - a(t)$, where $a(t)$ is a smooth path of self-adjoint operators on $L^2([0,\pi/2],\mathbb{C}^n)$. This completes the definition of a Cauchy-Riemann-type operator in the relative case.

In the correct functional analytic setup, all Cauchy-Riemann-type operators are Fredholm and hence the space $\Sigma(E)$ of Cauchy-Riemann-type operators on a given bundle E with fixed asymptotic data has a well-defined determinant bundle. (See [12] for more details about the definition of a determinant bundle.) Assume for now that all of the spaces $\Sigma(E)$ are orientable, i.e. that their determinant bundles are trivializable. Denote an orientation on $\Sigma(E)$ by $\sigma(E)$. Since we assume that $\Sigma(E)$ is orientable, it is enough to orient the determinant line over one operator $L \in \Sigma(E)$ to determine $\sigma(E)$. As a result, we will frequently abuse notation and refer to $\sigma(L)$ instead of $\sigma(E)$.

Following [8], we want to put a **coherent set of orientations** on all spaces of Cauchy-Riemann-type operators on bundles over Riemann surfaces with boundary. Such a set of orientations must satisfy three axioms:

Disjoint Union: Given bundles $E_j \to S_j$ for $j = 1,2$, define the **disjoint union bundle** $E_1 \sqcup E_2 \to S_1 \sqcup S_2$ by $(E_1 \sqcup E_2)|_{S_j} = E_j$. If we have operators $L_j \in \Sigma(E_j)$, then there is an operator L on $E_1 \sqcup E_2$ such that $L|_{H^{1,2}(E_j)} = L_j$. The determinant line $\det L$ is canonically isomorphic to $\det L_1 \otimes \det L_2$, and hence the orientations $\sigma(L_j)$ induce an orientation $\sigma(L_1) \otimes \sigma(L_2)$ on $\det L$. The disjoint union axiom tells us to use this orientation:

$$\sigma(L_1) \otimes \sigma(L_2) = \sigma(L). \tag{8.3}$$

Direct Sum: Given bundles $E, F \to S$ and operators $L \in \Sigma(E)$ and $K \in \Sigma(F)$, there is a canonically defined operator $L \oplus K \in \Sigma(E \oplus F)$. Once again, $\sigma(L)$ and $\sigma(K)$ induce an orientation $\sigma(L) \oplus \sigma(K)$ on $\det(L \oplus K)$. The direct sum axiom states that:

$$\sigma(L) \oplus \sigma(K) = \sigma(L \oplus K). \tag{8.4}$$

Cut and Paste: Let S be a disjoint union of one or more Riemann surfaces with punctures on the boundary. Let $E \to S$ be a bundle. Let $\gamma_j : [0,1] \to S, j = 1,2$ be real-analytic embeddings with disjoint images; if $\gamma_j(0) \neq \gamma_j(1)$, then both γ_1 and γ_2 must map $\{0,1\}$ to ∂S. Let $\Phi : E|_{\gamma_1} \to E|_{\gamma_2}$ be a vector bundle isomorphism covering $\gamma_2 \circ \gamma_1^{-1}$.

If we cut S along the curves γ_j, we obtain a surface $\bar{S}$ with corners that has (possibly additional) boundary components $\gamma_j^{\pm}$. The bundle E gives rise to a bundle $\bar{E} \to \bar{S}$. We can identify sections of E with sections $\bar{h}$ of $\bar{E}$ that satisfy the boundary condition

$$\bar{h}|_{\gamma_j^-} = \bar{h}|_{\gamma_j^+} \quad \text{for } j = 1,2. \tag{8.5}$$

In addition, the operator L induces an operator $\bar{L}$ that acts on the sections of $\bar{E}$ that satisfy the boundary conditions (8.5).

If we shuffle the boundary conditions so that they read:

$$\begin{aligned} \Phi\bar{h}|_{\gamma_1^-} &= \bar{h}|_{\gamma_2^+} \\ \bar{h}|_{\gamma_2^-} &= \Phi\bar{h}|_{\gamma_1^+}, \end{aligned} \tag{8.6}$$

then the sections satisfying (8.6) correspond to sections of a new bundle E' which is formed by identifying γ_1^+ to γ_2^- and γ_1^- to γ_2^+ on the base level and using Φ to

identify the bundles at the fiber level. The operator L also induces a new operator L' on the sections of E'.

The boundary conditions (8.5) and (8.6) may be connected by a path in the space of bundles with mixed Riemann- and Riemann-Hilbert-type boundary conditions. These boundary conditions induce a path of Cauchy-Riemann-type operators, whose determinant lines may be oriented by continuation. Thus, via this path, the operator L' gets an orientation $\sigma(L, \gamma_j, \Phi)$ from L. The cut and paste axiom states that:

$$\sigma(L, \gamma_j, \Phi) = \sigma(L'). \tag{8.7}$$

See [8] for more details, especially with regards to the cut and paste operation. The cut and paste operation in [8] was designed to replace the more limited gluing construction of [12]. What is important for us is that gluing is retained as a special case of cutting and pasting. To see this, suppose that operators in $\Sigma(E \to S_1)$ tend asymptotically to A_∞ at $+\infty$ near a boundary puncture x and that operators in $\Sigma(F \to S_2)$ tend asymptotically to A_∞ at $-\infty$ near a boundary puncture y. By a homotopy, we may assume that there is an operator $L \in \Sigma(E)$ that is constant for all $s > \rho - 1$ in local strip coordinates near x; similarly, assume that there is an operator $K \in \Sigma(F)$ that is constant for all $s < -\rho + 1$ in local strip coordinates near y. Choose paths $\gamma_1(t) = (\rho - 1, t)$ near x and $\gamma_2(t) = (-\rho + 1, t)$ near y. The cut and paste operation results in an operator $L\#K$ on the "boundary connected sum" of S_1 and S_2 that is equal to L on the old S_1 and K on the old S_2 as well as a constant operator on a strip. The operator $L\#K$ is precisely the one obtained from gluing in [12].

In [8], Eliashberg, Givental, and Hofer prove that there exists a coherent set of orientations on *closed* Riemann surfaces (with punctures). Further, this set of orientations is determined by the three axioms above and a choice of orientations on $\Sigma(S^2 \times \mathbb{C})$, $\Sigma(\mathcal{O}(1) \to S^2)$, and the operators associated to the $+\infty$ asymptotic data at punctures and the trivial vertical cylinder (or all asymptotic data at punctures); see [8]. For the relative case to work, we must also include an orientation on $\Sigma(E = D^2 \times \mathbb{C}, E^\partial = \partial D \times \mathbb{R})$ and the operators associated to asymptotic data at positive boundary punctures (as in 8.2) and the trivial vertical strip. However, the relative case does not work in general, since the spaces of Cauchy-Riemann-type operators — in particular, their boundary conditions — are not necessarily orientable.

We now specialize to the case of orientations for the relative contact homology of Legendrian knots in $(\mathbb{R}^3, \xi_0)$. Since Reeb field for the standard contact structure is invariant under translations, it should come as no surprise that every Reeb chord yields the same asymptotic data. More precisely, we get:

Lemma 8.2. *All asymptotic operators for $(\mathbb{R}^3, \xi_0)$ have the form*

$$A_\infty h(t) = -i\frac{\partial h}{\partial t}$$

with respect to the Hermitian trivialization $\{\partial_x, \partial_y + x\partial_z, \partial_\tau, \partial_z\}$.

This lemma follows from the definitions, the local model discussed in Section 7.2, and Theorem 7.11.

With this in mind, we set up some notation: the space of all Cauchy-Riemann-type operators on a $\mathbb{C}^2$-bundle over the boundary-punctured disk D^2_* with asymptotic data given by the Reeb chords $\{a, b_1, \ldots, b_n\}$ is denoted $\Sigma(a; b_1, \ldots, b_n)$. When Σ comes from an honest moduli space, the bundle $f^*(T\mathbb{R}^3 \times \mathbb{R})$ splits into $\mathbb{C} \oplus \mathbb{C}$, with the first factor coming from the contact structure and the second coming from the complex direction spanned by the Reeb orbit and the vertical direction. The boundary conditions for the first factor come from the

diagram of the knot K; we may regard them as a path Λ in $\mathbb{RP}^1$ with fixed endpoints. The boundary conditions are trivial for the second factor as they always point in the vertical direction. If $\Sigma(a; b_1, \dots, b_n)$ has such a splitting, then it is parametrized by triples (J, A, Λ). Each component of this space of triples is contractible,[2] so the determinant bundle over $\Sigma(a; b_1, \dots, b_n)$ is orientable.

In the next section, we will describe a system of coherent orientations for the moduli spaces involved in relative contact homology for the standard contact $\mathbb{R}^3$. We will not present a complete system; rather, we will only use the axioms to orient the spaces required for the definition of the differential ∂ on $\mathcal{A}$. In particular, we only use split bundles as above, so the spaces Σ will always be orientable. Using the Translation Theorem (7.7), we will translate the geometric considerations detailed above into a diagrammatic formulation of coherent orientations in the xy-plane.

8.2. **A Combinatorial Approach.** Recall that the Translation Theorem 7.7 asserts that all J-holomorphic curves in the symplectization $\mathbb{R}^3 \times \mathbb{R}$ can be represented as holomorphic maps of boundary-punctured disks into $\mathbb{R}^2$ whose boundary is sent into the diagram of K. Slightly rephrased, this means that the boundary of a J-holomorphic curve in the symplectization gives rise to an oriented loop in the diagram of K that is immersed except at finitely many points, which may be either branch points or corners. Any one loop encodes all of the boundary conditions (via pulling back TK) and asymptotic conditions (via local lifts near the corners) for a Cauchy-Riemann-type operator on a $\mathbb{C}^2$-bundle over D^2_*; in other words, a family of oriented loops is equivalent to a family of operators $\Sigma(a; b_1, \dots, b_n)$. Following Floer and Hofer, we will expand the families of loops under consideration and orient *all* families $\Sigma(a; b_1, \dots, b_n)$ of oriented loops $\gamma(s)$ in the diagram of K that are immersed except at finitely many points, which may be either branch points or corners.

We put coordinates on a family of loops with k branch points by numbering the branch points consecutively with respect to the given orientation of the loop. We view them as coordinates on the k-torus $\prod_k S^1$ (in general, these coordinates only lie in a subspace of the k-torus). For orientation purposes, two numberings are equivalent if they differ by an *even* cyclic permutation. An orientation on a loop with k boundary branch points is given by an ordered basis for $T_p(S^1)^k \oplus \mathbb{R}$, which we shall represent by the ordered set of vectors $\langle \pm v_1, \dots, \pm v_k, \pm \partial_\tau \rangle$ with $v_j \in T_p S^1$ agreeing with the orientation on the loop γ and $\partial_\tau \in T_p \mathbb{R}$.

Note that we may arbitrarily add a pair of branch points on a loop in $\Sigma(a; b_1, \dots, b_n)$ and still have a loop in $\Sigma(a; b_1, \dots, b_n)$. We will see below that the orientation is unaffected by such an addition. This is related to the fact that if a loop γ comes as the boundary of a J-holomorphic disk with n interior branch points and m boundary branch points then, as we move about the moduli space containing this disk, one of the interior branch points could migrate to the boundary where it spawns two boundary branch points. However, since the interior branch points have two degrees of freedom with a canonical complex orientation, we have a natural orientation associated to the two new boundary branch points.

The construction of a coherent system of orientations proceeds in three steps:

(1) Orient all families of loops with no corners.
(2) At each crossing, orient precisely one family of loops with a single corner and no branch points with $\langle \partial_\tau \rangle$.

[2]However, in higher dimensions, $\pi_2(\mathrm{Lagr}(\mathbb{C}^n))$ is non-trivial, and hence the space of triples is not contractible.

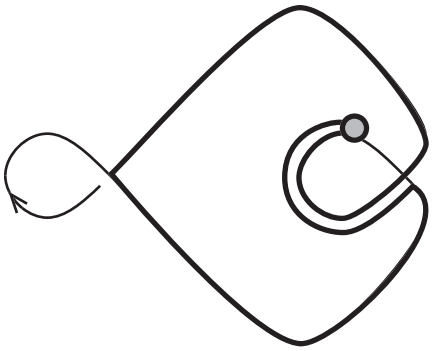

FIGURE 11. The xy projection of a (1+1)-dimensional moduli space. In this figure, and in all subsequent figures, the diagram of the knot K is designated by a thin line, while the image of an element in a moduli space is designated by a thick line.

(3) Every other family of loops gets oriented by gluing to families of loops from step 2 until there are no remaining corners and then comparing the result to the orientations from step 1.

To apply the cut-and-paste axiom we need to first choose an orientation for the trivial vertical strip. This is a dimension 0 object and will be oriented by $+1$. Now using the cut-and-paste axiom, the first step is equivalent to choosing orientations for operators on the trivial bundle $D^2 \times \mathbb{C}$ and on $\mathcal{O}(1)$. The second step mirrors a choice of orientation on a single asymptotic operator. See [8] for a similar procedure in the closed case.

Step 1. Any loop with no branch points or corners is related to an operator on a bundle that can be obtained from $D^2 \times \mathbb{C}$ and $\mathcal{O}(1)$ using the cut-and-paste axiom. We choose these orientations so that such a loop is oriented by $\langle \partial_\tau \rangle$. Examining our discussion above concerning the migration of interior branch points to the boundary yields the following convention for a loop Σ with k branch points and no corners: label each segment between two branch points in Σ by a '+' if the orientations of Σ and the knot K agree and by a '$-$' otherwise. We will refer to the order of signs before and after a branch point as its **alignment**. Starting with a branch point whose alignment is a $+$ then a $-$, number each branch point consecutively in the order encountered; this gives an ordering of the coordinates on Σ. The orientation is given by:

$$\langle v_1, v_2, \ldots, v_{k-1}, v_k, \partial_\tau \rangle . \tag{8.8}$$

This completes step 1.

Step 2. At each crossing, there are two families of loops without branch points and with exactly one corner. Orient one of them by $\langle \partial_\tau \rangle$. As we shall see below, it does not matter which, though for definiteness we assume that it is the family that goes around the quadrant about which the orientation of the knot runs counter-clockwise.

Step 3. The third and final step in constructing a coherent system of orientations relies on a diagrammatic understanding of the gluing process and its relationship with orientations. Let Σ and Σ' be families of loops that have corners at a common crossing. Suppose that Σ is oriented by $\langle v_1, \ldots, v_m, \partial_\tau \rangle$ and that Σ' is oriented by $\langle v'_1, \ldots, v'_n, \partial'_\tau \rangle$. Suppose further that loops in Σ go around a positive quadrant and loops in Σ' go around a

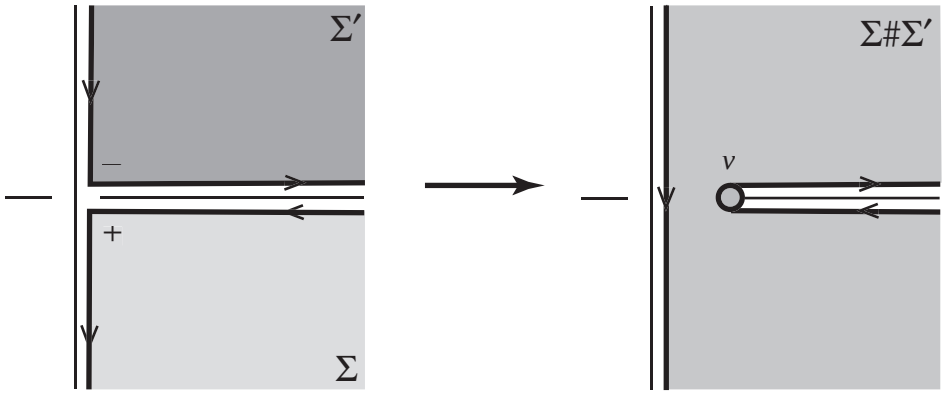

FIGURE 12. The gluing process as viewed in the xy projection. Note that α parametrizes the position of the branch point in the right-hand diagram.

negative quadrant.[3] In order to understand the orientation on the glued family of loops, we will examine what happens to the original families when we glue them together geometrically near the corners.

Diagrammatically, gluing Σ to Σ' creates a new branch point, as shown in Figure 12. We want to make this process analytically precise in the "straight line" model that we first examined in the proof of the Translation Theorem 7.7. In fact, it suffices to consider the straight line model since, after a homotopy, we may assume that the operators represented by the loops in Σ and Σ' come from the straight line model near the crossing. In this model, Σ is parametrized by the vertical translation factor $a \in \mathbb{R}$ and consists of the maps

$$f_a(u,v) : (u,v) \mapsto \left(e^{-u}\cos(v), -e^{-u}\sin(v), v, u + \frac{e^{-2u}}{2}\cos^2(v) + a \right). \tag{8.9}$$

Similarly, Σ' is parametrized by $a' \in \mathbb{R}$ and consists of the maps

$$f_{a'}(u,v) : (u,v) \mapsto \left(e^{u}\cos(v), e^{u}\sin(v), v, u + \frac{e^{2u}}{2}\cos^2(v) + a' \right). \tag{8.10}$$

We claim that the family of loops given locally by

$$F_{\alpha,\tilde{a}} : (u,v) \mapsto \Big(e^{-\alpha}\cosh(u)\cos(v), e^{-\alpha}\sinh(u)\sin(v), v, u + \frac{e^{-2\alpha}}{2}\cosh^2(u)\cos^2(v) + \tilde{a} \Big) \tag{8.11}$$

is the result of gluing Σ to Σ'. This family is parametrized by the pair $(\alpha, \tilde{a})$. The inverse of the gluing map is given locally by:

$$\Psi : (\alpha, \tilde{a}) \mapsto (\alpha + \tilde{a}, -\alpha + \tilde{a}). \tag{8.12}$$

The important point is that Ψ is orientation preserving, so the orientation on the glued family given by

$$\sigma(\Sigma)\#\sigma(\Sigma') = \langle v_1, \ldots, v_m, v_\alpha, v_1', \ldots, v_n', \partial_{\bar{\tau}} \rangle \tag{8.13}$$

is the correct one.

We now proceed to orient all remaining families of loops using the gluing procedure and the orientations chosen in steps 1 and 2 (and on the trivial strip). The idea is to start with a

[3]In other words, Σ lies "below" Σ' in the symplectization picture.

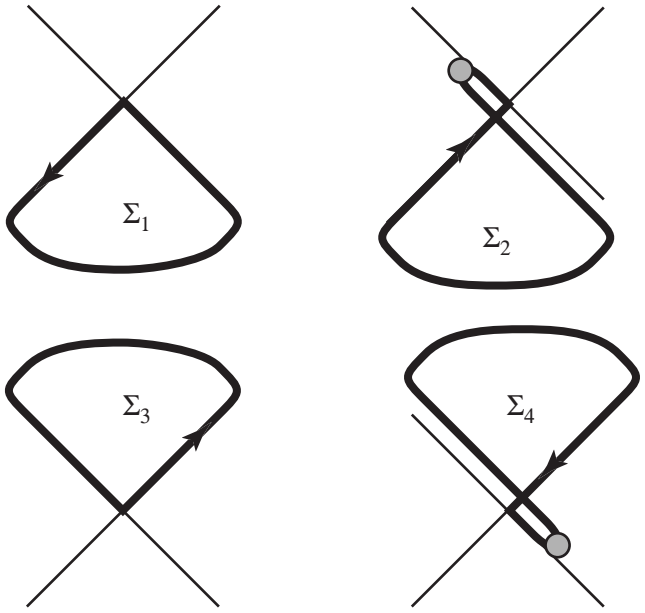

FIGURE 13. A list of the four loops that lie around a vertex. Each loop traverses half of K.

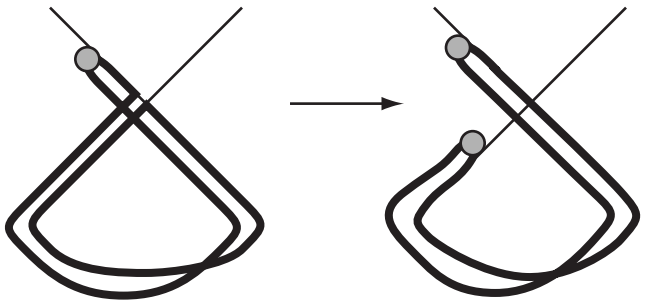

FIGURE 14. Gluing a basic loop to a $(1+1)$-dimensional loop with a corner at a '$-$'.

family of loops with corners, then glue to the families from step 2 until there are no corners left, and finally compare the result to the orientations in step 1.

First, we orient all of the families with one branch (or no) point(s) that lie around any given crossing (see Figure 13). For now, assume that the crossing in question is coherent about a $+$ (see Section 3.1). Glue Σ_1 to Σ_2, as pictured in Figure 14. If we orient Σ_2 with $\langle \pm w, \partial_\tau \rangle$, then the glued loop is oriented by $\langle v, \pm w, \partial_\tau \rangle$. Observe that v does not have the proper alignment to be listed first. The orientation for the corner-free family in step 1 is $\langle w, v, \partial_\tau \rangle$, so, upon comparison, the orientation $\sigma(\Sigma_2)$ must be $\langle -w, \partial_\tau \rangle$.

Orient the family Σ_4 using the same procedure as above. The resulting orientation is $\langle w, \partial_\tau \rangle$.

Finally, to check that the choice of coherent quadrant in step 2 does not matter, glue Σ_2 to the top family Σ_3, as shown in Figure 15. If we orient Σ_3 by $\langle \pm \partial_\tau \rangle$, then the glued family is oriented by $\langle \pm v, -w, \partial_\tau \rangle$. Since alignment considerations show that the appropriate orientation on the (2+1)-dimensional vertex-free family from step 1 is $\langle w, v, \partial_\tau \rangle$,

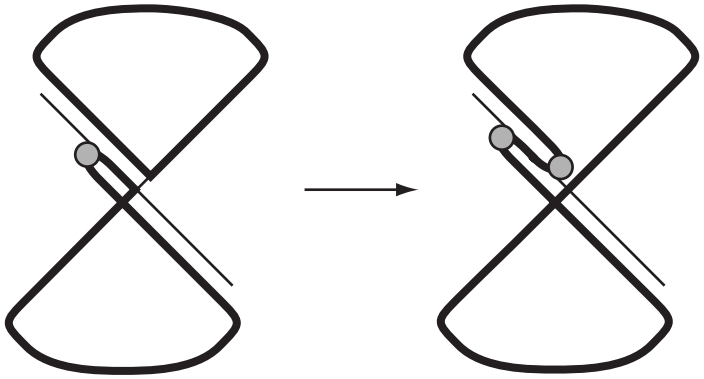

FIGURE 15. Gluing the $(1+1)$-dimensional loop with a corner at a '$-$' to the loop opposite the basic loop.

the orientation on Σ_3 should be $\langle \partial_\tau \rangle$. That this is the same orientation as for Σ_1 comes from the fact that Σ_1 and Σ_3 represent the same family of operators.

So far, we have oriented all families with one corner at a vertex that is coherent about a $+$. To orient families around a vertex that is coherent about a $-$, we follow exactly the same procedure, taking care to use the "bottom-to-top" order of gluing. As a result, the signs on the vector w for the loops covering the incoherent quadrants are reversed: $\langle w, \partial_\tau \rangle$ for the leftmost (outward-pointing) family Σ_2 and $\langle -w, \partial_\tau \rangle$ for the rightmost (inward-pointing) family Σ_4. On the other hand, both $(0+1)$-dimensional families are still oriented by $\langle \partial_\tau \rangle$.

In the general case, we consider a family of loops Σ with positive corners labeled by $i_1, \dots, i_m$ (in a cyclic order) and negative corners labeled by $j_1, \dots, j_n$. Suppose that Σ has an orientation given by

$$\sigma(\Sigma) = \langle v_1, \dots, v_a, \pm\partial_\tau \rangle \,. \tag{8.14}$$

Our task is to determine the sign on ∂_τ that will fit $\sigma(\Sigma)$ into a coherent system of orientations. At each crossing i_j, glue in one of the families Σ_i. After gluing to all of the corners, we are left with a family that has no corners and an orientation given by:

$$\sigma(\Sigma_{i_m}) \# \cdots \# \sigma(\Sigma_{i_1}) \# \sigma(\Sigma) \# \sigma(\Sigma_{j_1}) \# \cdots \# \sigma(\Sigma_{j_n}).$$

Compare this orientation to the orientation constructed in step 1 and choose the sign of ∂_τ so that the two orientations agree. This completes step 3.

8.3. **The Algorithm for Dimension $(0+1)$ Disks.** In this section, we explain how to obtain signs for dimension $(0+1)$ families of loops that represent immersed disks. Our goal is to translate the gluing process in the previous section into a concrete, computable algorithm that, as expected, depends only on contributions from the corners. We get an actual sign rather than just an orientation for the family $\Sigma(a; b_1, \dots, b_k)$ by comparing the orientation $\sigma(\Sigma)$ with the "flow orientation" $\langle \partial_\tau \rangle$. Specifically, we show:

Theorem 8.3. *The sign on a holomorphic disk $f \in \mathcal{M}^A/\mathbb{R}$ in a moduli space of dimension $(0+1)$ given by comparing the coherent orientation on f and the "flow orientation" is the same as the sign on $p(f) \in \Delta^A$ described in Definition 3.5.*

The remainder of this section is devoted to the proof of this theorem.

Our analysis begins with step 3 of the previous section. The idea is to look at the contributions that come from gluing to each corner individually. The order in which we

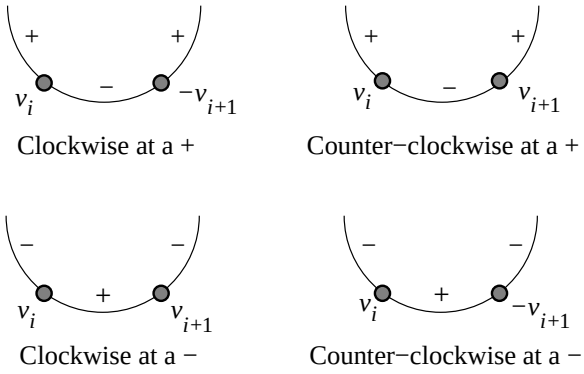

FIGURE 16. Orientation choices at coherent vertices, pulled back to S^1 for clarity.

glue depends on the counter-clockwise cyclic order in the corners, i.e. we start with a and end up with b_k. At a coherent corner, gluing gives two new vectors in the orientation (see Figure 15, for example); at an incoherent corner, gluing gives only one new vector.

At a coherent corner of either sign, the sign contribution depends on the number of negative vectors added during the gluing process. If there is one negative vector, then, ignoring alignment for the moment, we need to flip a single sign to make the pair agree with the base orientation from step 1. Thus, there is a sign contribution of -1 in this case. On the other hand, the same reasoning shows that there is no sign contribution when the coherent corner contributes an even number of negative vectors. See Figure 16 for the vectors given by the conventions adopted in the previous section. It follows from Figure 16 that corners that are clockwise at a '+' and counter-clockwise at a '−' pick up a negative sign.

Incoherent corners come in inward / outward pairs. Our analysis of gluing shows that each pair contributes two positive vectors. Hence, by the same analysis as in the coherent case, there is no sign contribution at an incoherent corner.

Finally, we consider alignment issues. Suppose that the positive corner, a, is either clockwise coherent or inward-pointing. On the first segment of the loop, the orientation of the knot disagrees with the counter-clockwise orientation of the family. Since we agreed to start labeling the branch points with one that changes alignment from + to −, we have to take into account a cyclic permutation of the labelings. This is an *odd* permutation since a cornerless family of loops has an even number of branch points. Thus, we pick up an extra negative sign at a + vertex when it is either clockwise coherent or inward-pointing.

In sum, we have deduced that Definition 3.5 assigns the correct sign to a dimension $(0+1)$ disk.

Note that there are actually sixteen different sets of choices for the signs in Figure 3. This is reflected by the orientations we chose in Section 8.1 on $D^2 \times \mathbb{C}$, $\mathcal{O}(1)$, the capping disk without branch points, and the trivial vertical strip. It turns out that all of the orientation choices give the same DGA, possibly after replacing some generators by their negatives.

9. Acknowledgments

We would like to thank Yasha Eliashberg and Frederic Bourgeois for many stimulating discussions about the material presented in this paper. In addition, we would like to thank the American Institute of Mathematics (AIM) for facilitating the Low-Dimensional Contact Geometry program, during which we completed this work.

References

[1] C. Abbas. Finite energy surfaces and the chord problem. *Duke Math. J.*, 96:241–316, 1999.
[2] B. Aebischer et al. *Symplectic Geometry*, volume 124 of *Prog. Math.* Birkhäuser, 1994.
[3] D. Bennequin. Entrelacements et equations de Pfaff. *Asterisque*, 107–108:87–161, 1983.
[4] R. Bott and L. Tu. *Differential Forms in Algebraic Topology*, volume 82 of *Graduate Texts in Mathematics*. Springer-Verlag, 1982.
[5] F. Bourgeois. Private correspondence.
[6] Yu. Chekanov. Differential algebra of Legendrian links. *Invent. Math.*, 150:441–483, 2002.
[7] Y. Eliashberg and M. Fraser. Classification of topologically trivial Legendrian knots. In *Geometry, topology, and dynamics (Montreal, PQ, 1995)*, pages 17–51. Amer. Math. Soc., Providence, RI, 1998.
[8] Y. Eliashberg, A. Givental, and H. Hofer. Introduction to symplectic field theory. *Geom. Funct. Anal.*, (Special Volume, Part II):560–673, 2000. GAFA 2000 (Tel Aviv, 1999).
[9] J. Etnyre and K. Honda. On the non-existence of tight contact structures. *Ann. Math. (2)*, 153:749–766, 2001.
[10] J. Etnyre and K. Honda. Knots and contact geometry. *J. Symplectic Geom.*, 1(1):63–120, 2002.
[11] J. Etnyre and K. Honda. Tight contact structures with no symplectic fillings. *Invent. Math.*, 148(3):609–626, 2002.
[12] A. Floer and H. Hofer. Coherent orientations for periodic orbit problems in symplectic geometry. *Math. Z.*, 212:13–38, 1993.
[13] D. Fuchs and S. Tabachnikov. Invariants of Legendrian and transverse knots in the standard contact space. *Topology*, 36:1025–1053, 1997.
[14] H. Hofer, K. Wysocki, and E. Zehnder. Properties of pseudoholomorphic curves in symplectizations. III. Fredholm theory. In *Topics in Nonlinear Analysis*, pages 381–475. Birkhäuser, Basel, 1999.
[15] Y. Kanda. The classification of tight contact structures on the 3-torus. *Comm. Anal. Geom*, 5:413–438, 1997.
[16] P. B. Kronheimer and T. S. Mrowka. Monopoles and contact structures. *Invent. Math.*, 130(2):209–255, 1997.
[17] P. Lisca and G. Matic. Stein 4-manifolds with boundary and contact structures. *Topology Appl.*, 88:55–66, 1998.
[18] J. Robbin and D. Salamon. The Maslov index for paths. *Topology*, 32:827–844, 1993.
[19] J. Robbin and D. Salamon. Asymptotic behavior of holomorphic strips. *Ann. Inst. H. Poincaré Anal. Non Linéaire*, 18:573–612, 2001.
[20] L. Rudolph. An obstruction to sliceness via contact geometry and "classical" gauge theory. *Invent. Math*, 119:155–163, 1995.

Stanford University, Stanford, CA 94305
E-mail address: etnyre@math.stanford.edu
URL: http://math.stanford.edu/~etnyre

Massachusetts Institute of Technology, Cambridge, MA 02139
E-mail address: lenny@math.mit.edu
URL: http://math.mit.edu/~lenny

Stanford University, Stanford, CA 94305
E-mail address: sabloff@math.stanford.edu
URL: http://math.stanford.edu/~sabloff